LOW-COST BLIND CARRIER FREQUENCY OFFSET ESTIMATOR FOR MIMO MULTICARRIER SYSTEMS

LI MI

NATIONAL UNIVERSITY OF SINGAPORE

2005

LOW-COST BLIND CARRIER FREQUENCY OFFSET ESTIMATOR FOR MIMO MULTICARRIER SYSTEMS

LI MI

(B. Eng, SJTU)

A THESIS SUBMITTED

FOR THE DEGREE OF MASTER OF ENGINEERING

DEPARTMENT OF ELECTRICAL AND COMPUTER ENGINEERING

NATIONAL UNIVERSITY OF SINGAPORE

2005

Acknowledgements

I would like to express my sincere thanks to my supervisors, Professor Nallanathan Arumugam and Professor Attallah Samir, for their invaluable guidance, support, encouragement, patience, advice and comments throughout my research work and this thesis.

Special thanks to my parents, who always encourage, support and care for me throughout my life.

I also wish to give my thanks to all the students and staff in Communications Lab and ECE-I2R Wireless Communications Lab for their discussion and friendship.

I am grateful for research scholarship from the National University of Singapore for giving me the opportunity to carry out my research work.

Contents

List of Figures

List of Abbreviations

1G	The first generation wireless systems
2G	The second generation wireless systems
3G	The third generation wireless systems
4G	The fourth generation wireless systems
AWGN	Additive White Gaussian Noise
BER	Bit Error Rate
CFO	Carrier Frequency Offset
CIR	Carrier-to-Interference Ratio
CP	Cyclic Prefix
CRLB	Cramér-Rao Lower Bound
FFT	Fast Fourier Transform
FWA	Fixed Wireless Access
GSM	Global System Mobile
HIPERLAN	High Performance European Radio LAN
IBI	Inter-Block Interference
ICI	Inter-Channel Interference
ICI	Inter-Carrier Interference
IDFT	Inverse Discrete Fourier Transform
IFFT	Inverse Fast Fourier Transform
ISI	Inter-Symbol Interference
LOS	Line of Sight
MC	Multi-Carrier
MC-CDMA	Multi-Carrier Code Division Multiple Access
MCM	Multi-Carrier Modulation
MIMO	Multi-Input Multi-Output
ML	Maximum Likelihood
MMAC [3]	Multimedia Mobile Access Communication
MSE	Mean Square Error
MTS	Mobile Telephone System
OFDM	Orthogonal Frequency Division Multiplexing
PANs	Personal Area Networks
PLL	Phase-Locked Loop
PSK	Phase Shift Keying
QAM	Quadrature Amplitude Modulation
QPSK	Quadrature Phase Shift Keying
RF	Radio Frequency
SISO	Single-Input Single-Output
SNR	Signal Noise Ratio
S/P	Series to Parallel
STBC	Space-Time Block Codes
STTC	Space-Time Trellis Codes
V-BLAST	Vertical-Bell Laboratories layered space-time

VCO	Voltage-Controlled Oscillator
WLANs	Wireless Local Access Networks

List of Symbols & Notations

$\mathbf{c}_\nu$	The spreading code
$\mathbf{C}$	The spreading matrix
$\mathbf{D}_N(\omega)$	The $P \times P$ diagonal matrix defined as $\mathbf{D}_N(\omega) \coloneqq \mathbf{D}_N(\mathbf{f}_N(\omega))$
$f(\mathbf{Y}, \omega_0)$	The log-likelihood function
$\mathbf{F}_N^H$	$N \times N$ IFFT matrix
$\mathbf{h}$	The discrete-time finite impulse response of channel
$\mathbf{H}$	The channel matrix
$\overline{i_k}$	The indices of the information symbols
i_k	The indices of the inserted zeros
$\mathbf{I}_N$	The $N \times N$ identity matrix
$J(\omega)$	The cost function
K	The number of information symbols in each block
L	The channel order
M	The number of blocks used to estimate the covariance matrix
N	The number of symbols in each block after null subcarrier insertion
N_r	The number of receive antennas
N_s	The total number of Monte Carlo trials
N_t	The number of transmit antennas
N_u	The number of users
P	The transmitted block size
$\mathbf{R}_{CP}$	The CP removing matrix
$\mathbf{R}_{\mathbf{yy}}$	The covariance matrix
$\mathbf{s}(k)$	The $k-th$ block of the information stream
$\mathbf{T}_{SC}$	The null subcarrier insertion matrix
$\mathbf{T}_{ZP}$	The zero-padding matrix

$\mathbf{T}_{CP}$	The CP insertion matrix
$\mathbf{y}(k)$	The IBI-free received block
ω	The candidate carrier frequency offset estimate
ϖ	The subcarrier spacing
ω_0	The normalized carrier frequency offset
$\hat{\omega}_0$	The estimated carrier offset
$\eta(i)$	Additive white Gaussian noise (AWGN)
$\mathcal{J}(\omega_0)$	The Fisher's information matrix (FIM)
$\Im[\cdot]$	The imaginary part of a complex number
$\Re[\cdot]$	The real part of a complex number
$E[\cdot]$	The expectation with respect to all the random variables within the brackets

Summary

Multicarrier modulation is a promising technique that can be used for high speed data communications. In multicarrier systems, the symbols are transmitted in parallel over a number of lower rate subcarriers. Because the channel is converted into a set of parallel narrowband frequency-flat fading subchannels, multicarrier system is robust against frequency selective fading. A guard time interval is inserted to eliminate the inter-symbol interference (ISI).

For the high data rate required by next generation wireless systems, multi-input multi-output (MIMO) transmission over multi-antennas is a promising technique that can satisfy the demand. MIMO techniques can be implemented in many different ways to improve the power efficiency and capacity of communication systems.

Orthogonal frequency division multiplexing (OFDM) is a typical form of multicarrier modulation. In an OFDM system, any frequency offset will cause the loss of orthogonality between the subcarriers resulting in inter-channel interference (ICI) and ISI. Three major causes of ICI and ISI are phase noise, frequency offset and timing errors. In this thesis, we consider the sensitivity of OFDM to carrier frequency offset (CFO). Bit error rate (BER) analysis of OFDM shows that the presence of CFO causes great degradation in the performance.

In the literature, many estimation schemes have been proposed to estimate the CFO. They can be classified into two groups: data-aided and blind. Data-aided

schemes use pilot symbols, repeated symbols or training symbols to estimate the CFO, whereas the blind estimators make use of the special characteristics of received symbols, such as cyclic prefix, correlation of received signals, phase shift, null subcarriers and so on.

In this thesis, we propose a blind CFO estimator which makes use of the null subcarriers in a multicarrier system. Firstly, we present a high-cost blind CFO estimation algorithm which makes use of null subcarriers. Then we improve the method using Taylor's series expansion. Considering the identifiability problem, the null subcarriers are inserted with distinct spacings. The numerical results show that the proposed method can reduce the computational cost significantly without sacrificing the performance. In addition, we extend the proposed method from single-input single-output (SISO) multicarrier systems to MIMO multicarrier systems. Cramér-Rao lower bound and theoretical mean square error (MSE) are derived to measure the performance of the estimator. We also analyze the reduction of the computational cost due to the new method in detail. The contributions above led to three publications listed at the end of the thesis.

Chapter 1
Introduction

In the past century, wireless communication technologies have developed greatly. Nowadays, new personal wireless communication methods and devices are developed and adopted by the people throughout the world, making communication between any two places convenient. Especially in the last decade, rapid development of new technologies, such as digital and radio frequency (RF) circuit fabrication and new large-scale circuit integration, has made the devices smaller, cheaper and affordable to most people. In the future, a technology which can provide high data rate is required for the development of 3G systems and wireless local area network (WLANs). Since the radio spectrum resources are limited, new modulation methods and system structures are the key to enhance the capability of wireless communication systems.

1.1 Wireless Communication

Wireless communication systems have developed rapidly during the past 100 years [1]. In 1946, Mobile Telephone System (MTS), which was the first public mobile telephone system, was constructed in United States [2]. Although the mobile transceivers were bulky, MTS was a milestone in the history of wireless communications.

MTS had its limitations and provided only small capacity, so the number of users could not grow rapidly. In 1960s, the cellular concept was developed by AT&T Bell Laboratories, which made the prevalence of mobile phone in real life [2]. Since then, the number of wireless customers throughout the world has increased to one billion. In early 1980s, the first generation of cellular systems (1G) was developed. They were analog systems, and were able to provide wireless services in many countries [2]. By late 1980s, the digital technique, which was adopted by the second generation of cellular systems (2G), was employed to alleviate the disadvantages of the earlier analog systems. From early 1990s to present, Global System Mobile (GSM) is the most popular 2G standard in the world [2]. Nowadays, the third generation wireless systems (3G), which can provide both voice and high bit-rate data services, is the new direction of wireless communications development.

Wireless data systems are another important area of wireless communication. The first wireless data system, known as ALOHA, was developed in 1971. There are many types of wireless data systems: Wide Area Data Systems, WLANs, Wireless ATM and Personal Area Networks (PANs) [2]. Among these systems, WLANs, which are used to transmit high-speed data in a small region, are the most important. In the past decades, many standards have been developed for WLANs. In USA, the IEEE 802.11 WLANs working group proposed two important standards: 802.11a and 802.11b. Another WLANs standard, high performance European Radio LAN (HIPERLAN) is popular in Europe [1].

From the history of wireless communications, we can see that the trend of

development tends towards support for advanced data services. The fourth generation (4G) systems are expected to provide high data rates from 50 Mbps to 155 Mbps [2]. In the course of development, there are many issues that must be resolved, among which the technical problems are the most important ones.

1.2 Multicarrier Systems

In order to support high data rates in 4G systems, more efficient modulation techniques are required. Multicarrier (MC) modulation is the one which can meet this requirement and is considered for 4G systems [3]. In multicarrier systems, the high rate data stream is split into several lower rate data streams. The channel bandwidth is also divided into many narrowband sub-channels. All parts of the messages are simultaneously transmitted over a number of lower rate subcarriers [4].

Besides high spectral efficiency, another advantage of multicarrier systems is that they are robust against frequency selective fading. It is because the channel is converted into a set of parallel narrowband frequency-flat fading subchannels [5] [6]. Time-guard or cyclic prefix is added to eliminate the inter-symbol interference (ISI) [6].

Orthogonal frequency division multiplexing (OFDM), which is a typical case of multicarrier system, has been adopted by many standards (e.g. IEEE 802.11a, IEEE 802.11g, and HIPERLAN/2). MC-CDMA, which is the combination of OFDM and code division multiple access (CDMA), has attracted much attention for its ability to transmit multiple users' data over a set of narrowband carriers [4]. These two types of

systems are seen as the promising techniques for the wireless communication of future [7].

1.3 MIMO Systems

For the fourth (and beyond) generation wireless systems, new transmission techniques are expected to support up to 100 Mbps for mobile telephone and up to 1 Gbps for WLANs. Multi-input multi-output (MIMO) transmission over multi-antennas is considered to be one of the promising techniques that can satisfy the demand for high data rate [8]. A MIMO system takes advantage of the spatial diversity obtained by spatially separated antennas in a dense multipath scattering environment [9]. MIMO systems have been implemented in many different ways to obtain either a diversity or capacity gain [10].

In general, MIMO techniques can be classified into three types. Improving the power efficiency by maximizing spatial diversity is the aim of the first type of techniques, which includes delay diversity, space-time block codes (STBC) [11] and space-time trellis codes (STTC) [12]. The second class uses a layered approach to increase capacity. One of the examples is Vertical-Bell Laboratories layered space-time (V-BLAST) architecture [13]. The last type exploits the knowledge of channel at the transmitter [9].

Since it has been demonstrated that the capacity and bit error rate can be enhanced significantly in MIMO systems [8], the commercial value of this technique has received much attention. Studies on it are progressing rapidly, and it has been

proposed in some standards. MIMO architectures are expected to be the key in the development of broadband fixed wireless access (FWA) and WLANs [14].

1.4 Importance of Carrier Frequency Offset Estimation

In a multicarrier system, it is very important that the subcarriers are orthogonal to each other, or the inter-carrier interference (ICI) will degrade the performance of the system. Thus, the removal of phase noise, frequency offset and timing errors, which are the three major causes for the loss of orthogonality, is a critical step at the receiver.

In this thesis, we will focus on the estimation of carrier frequency offset (CFO). CFO is caused by misalignment in carrier frequencies, which is due to imperfect oscillators and Doppler shift. These imperfections will destroy subcarrier orthogonality and introduce ICI in addition to attenuation and rotation of each subcarrier. BER analysis of OFDM shows that the presence of CFO causes great degradation in performance [15].

In order to estimate and eliminate the CFO accurately, many different estimation methods have been proposed in the past decade. The two major classifications of these CFO estimators are data-aided, which often use pilot or training symbols to estimate the CFO, and non-data-aided (blind), which make use of the received symbols only. There are many different methods in each class. For example, one kind of blind estimator, which is discussed in this thesis, makes use of the null subcarriers in the system [16]. Because of high computational cost and identifiability problem of this algorithm, we make an improvement to resolve these problems, and extend it to

MIMO multicarrier systems.

1.5 Organization & Contribution of the Thesis

In this thesis, we present a low-cost blind estimator for multicarrier system based on the following considerations: 1) In multicarrier systems, CFO is usually divided into integer part and fractional part. 2) In a digital system, the synchronization will usually be done as a 2-step approach. First, the integer part (coarse) of CFO is detected and compensated in the analog part. Then, in the digital part, only fine residual CFO has to be estimated. Thus, we assume that CFO $|\omega_0| \ll 1$. The proposed algorithm is based on the use of null subcarriers and the orthogonality among the columns of inverse fast Fourier transform (IFFT) matrix.

In Chapter 1, the development of wireless communications is introduced. The concepts and advantages of the multicarrier and MIMO systems are also introduced.

An overview on multicarrier systems is presented in Chapter 2. Two most typical cases of multicarrier systems, viz. OFDM and MC-CDMA, are described in detail. The basic concepts and advantages are also discussed.

In Chapter 3, the importance of synchronization in multicarrier systems is emphasized. The harm that CFO does to multicarrier systems is described. Different methods are provided to estimate the CFO. These methods are classified into two main categories: data-aided and non-data-aided. The advantages and disadvantages of the two types are discussed.

In Chapter 4, a low-cost CFO estimation method for multicarrier systems is

proposed. The identifiability problem is also considered. Null subcarriers are inserted with distinct spacings to ensure unique minimum of the cost function. In the simulation part, the method is compared with a high-cost CFO estimator, and the results show that the performance is comparable.

In Chapter 5, the low-cost estimation algorithm is extended to MIMO multicarrier systems. Then two criteria, Cramér-Rao lower bound (CRLB) and theoretical MSE, are derived to evaluate the performance of the estimator. The computational complexity of the proposed method is compared with an existing method in detail, and the reduction of the cost is significant. In the simulation part, the results under different situations show that the MIMO systems have better performance than single input single output (SISO) systems. The relationship between the parameters in the cost function and CFO is also discussed.

In Chapter 6, conclusions are drawn from the theoretical analysis and simulation results shown in the preceding chapters. Recommendations for future work are also included.

In this thesis, we improve an existing blind CFO estimation algorithm with high computational cost to a low-cost estimator for multicarrier systems. Then, the proposed estimator is extended to the MIMO multicarrier systems, specifically, MIMO OFDM and MIMO MC-CDMA. By comparing to the CRLB and theoretical MSE, and analyzing the cost reduction, we show that the proposed method reduces the computational complexity significantly without sacrificing the performance.

Chapter 2

Overview of Multicarrier Systems

2.1 Introduction

In the next generation of wireless communication systems, demands on data rates will exceed 100 Mbps. In order to support the high data rates, new spectrum efficient air interfaces must be introduced. Multicarrier systems can meet such requirements.

Orthogonal Frequency Division Multiplexing (OFDM) is a typical form of multicarrier modulation. The basic principle of OFDM is to divide the available spectrum into a number of narrowband subcarriers. Since the message is sent in parallel over a number of low-rate subcarriers, the symbol duration increases and the relative amount of dispersion in time caused by multipath delay spread is decreased. Therefore, OFDM systems are robust to frequency-selective fading, and the inter-symbol interference (ISI) can be eliminated by a simple insertion of a cyclic prefix.

However, OFDM systems are used for single-user communications. Therefore, another important type of multicarrier system, known as MC-CDMA, has also received much attention. It is the combination of OFDM and CDMA systems. Besides having all the merits of OFDM systems, MC-CDMA systems can be used for multi-user communications.

2.2 History of Multicarrier Systems

In late 1950s and early 1960s, multicarrier modulation (MCM) was first employed in military HF radio links, such as KINEPLEX [17] and KATHRYN [18]. Because the control of frequencies of subcarrier local oscillators and the detection of subcarrier signals with analog filters were not precise enough at that time, nonoverlapped band-limited orthogonal signals were used in the systems [3]. But the concept of employing time-limited orthogonal signals, which is the same as current OFDM, was proposed in 1960 [19].

In order to employ overlapped band-limited orthogonal signals in multicarrier systems, many studies were carried out in the 1960s. The name of “OFDM” first appeared in the U. S. Patent No.3 issued in 1970 [20]. Since then, the research on MCM has developed very rapidly. The applications of OFDM have been extended to telephone networks, digital audio broadcasting and digital television terrestrial broadcasting [3]. Furthermore, OFDM has been adopted by many standards, such as IEEE 802.11a, HIPERLAN/2 and multimedia mobile access communication (MMAC).

2.3 OFDM Systems

2.3.1 Principles of OFDM

The concept of OFDM is to transmit the data through a number of spectrally overlapped subcarriers which are modulated by phase shift keying (PSK) or quadrature amplitude modulation (QAM). Therefore, the most important part is to

arrange the subcarriers with appropriate spacing so that the signals can be received without adjacent carrier interference, which means that the subcarriers must be orthogonal to each other. In other words, if the symbol period of the individual signal is T_s, the subcarrier spacing must be chosen as a multiple of $1/T_s$ to ensure the orthogonality of the subcarriers. Fig. 2.1(a) shows an individual signal spectrum of an OFDM subcarrier with symbol period T_s, while Fig. 2.1(b) is an OFDM signal spectrum with subcarrier spacing $1/T_s$ [15]. It is clear that there is no interference from other subchannels at the center frequency of each subcarrier.

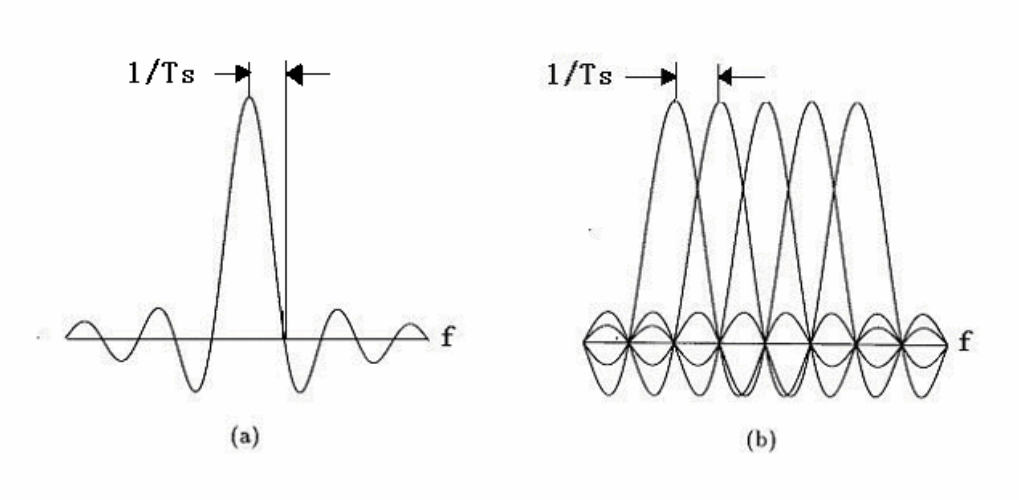

Fig. 2.1 (a) An individual signal spectrum. (b) OFDM signal spectrum

Since an OFDM signal consists of a sum of subcarriers, we set the original complex-valued data on the $n-th$ subcarrier as $d_n = a_n + jb_n$, and the mathematical expression of the signal is [24]

$$X(t_m) = \sum_{n=0}^{N-1} (a_n \cos \omega_n t_m + b_n \sin \omega_n t_m) \tag{2.1}$$

where a_n and b_n are the in-phase and quadrature terms, respectively, of the QAM/PSK signal, $\omega_n = 2\pi n/(N\triangle t)$ is the subcarrier frequency, N is the number

of subcarriers, $t_m = m\triangle t$, and $\triangle t$ is the symbol duration of the input serial data d_n.

For a large number of subcarriers, direct generation and demodulation of OFDM signal requires arrays of coherent sinusoidal generators that become unreasonably complex and expensive. However, we note that equation (2.1) is actually the real part of the Inverse discrete Fourier transform (IDFT) of the original data d_n [25], i.e.

$$\begin{aligned} X(t_m) &= \Re\{\sum_{n=0}^{N-1}(a_n + jb_n)\cdot \exp(-j\omega_n t_m)\} \\ &= \Re\{\sum_{n=0}^{N-1}(a_n + jb_n)(\cos\omega_n t_m - j\sin\omega_n t_m)\} \\ &= \sum_{n=0}^{N-1}(a_n \cos\omega_n t_m + b_n \sin\omega_n t_m) \end{aligned} \tag{2.2}$$

where $\Re(\bullet)$ denotes the real part of a complex number. From equation (2.2), we can find that there are N subcarriers with each one carrying one symbol from the original data d_n, and subcarrier spacing is $1/(N\triangle t)$. The inverse of the subcarrier spacing, $T = N\triangle t$, is defined as the OFDM symbol duration, which is N times longer than that of the original data symbol duration $\triangle t$ [24].

Substituting $\omega_n = 2\pi n/T = 2\pi n/(N\triangle t)$ in (2.2), we get

$$x(m) = \sum_{n=0}^{N-1} d_n \exp(j\frac{2\pi mn}{N}). \tag{2.3}$$

Since IDFT is used to implement the OFDM modulation, the original PSK/QAM data d_n is said to be in the frequency domain, while the OFDM signal $x(m)$ is in the time domain. In practice, the IDFT can be implemented via the fast Fourier transform (FFT) algorithm, which is more computationally efficient [26].

2.3.2 Guard Interval and Cyclic Prefix

If there is no transmission channel distortion in the system, the orthogonality of subcarriers in OFDM can be maintained and individual subcarriers can be separated completely and demodulated by FFT at the receiver. Due to linear distortions, such as multipath delay and micro-reflection, each symbol may spread its energy to the adjacent subcarriers, which introduces inter-symbol interference (ISI) between OFDM symbols. Furthermore, ISI can cause loss of orthogonality and the effect is similar to co-channel interference [27]. However, when delay spread is small, the impact of ISI is insignificant.

To eliminate ISI completely, a guard interval is introduced for each OFDM symbol. The total symbol duration then becomes $T_{total} = T_g + T_s$, where T_g is the time guard interval and T_s is the useful symbol duration. The extended guard time chosen is larger than the expected delay spread, so that multipath components from one OFDM symbol cannot interfere with the next one [15]. Since the insertion of guard intervals will reduce data throughput, T_g is usually less than $T_s / 4$ [24].

In practical systems, each OFDM symbol is preceded by a periodic extension of the signal itself in the guard time, which is known as cyclic prefix. This ensures that delayed replicas of the OFDM symbol always have an integer number of cycles within the FFT interval and ICI problem will not arise, as long as the delay is smaller than the guard time [15].

2.3.3 Complete system model for OFDM

Fig. 2.2 shows a block diagram of a complete OFDM system [15]. At the transmitter, binary input data is first encoded by a forward error correction code. The encoded data is interleaved and mapped onto QAM/PSK symbols. Then pilot symbols, which will be used for the synchronization at the receiver, are inserted into the blocks. After passing through the serial to parallel converter, the information blocks are modulated by IFFT and then converted back to serial. At last, the symbol sequence is sent out after the cyclic prefix insertion, and the digital-to-analog conversion.

In the receiver, the process is almost the reverse. But there are also some different steps from the transmitter. Before the cyclic prefix removal, the timing and frequency offset must be estimated and compensated. The estimation of channel has to be done to ensure that the demapping of the QAM signals is accurate.

2.4 MC-CDMA Systems

In OFDM systems, once a subcarrier is allocated to a given user, the other users cannot use that subcarrier until it is released from the user who occupies it. It means that the OFDM systems can serve only one user at one time. In 1993, MC-CDMA, which can provide service for a number of users simultaneously, was proposed independently [21-23]. Since then, MC-CDMA has drawn a lot of attention, and many studies have been done on it. Now, MC-CDMA system is considered to be one of the candidates as a physical layer protocol for 4G mobile communications.

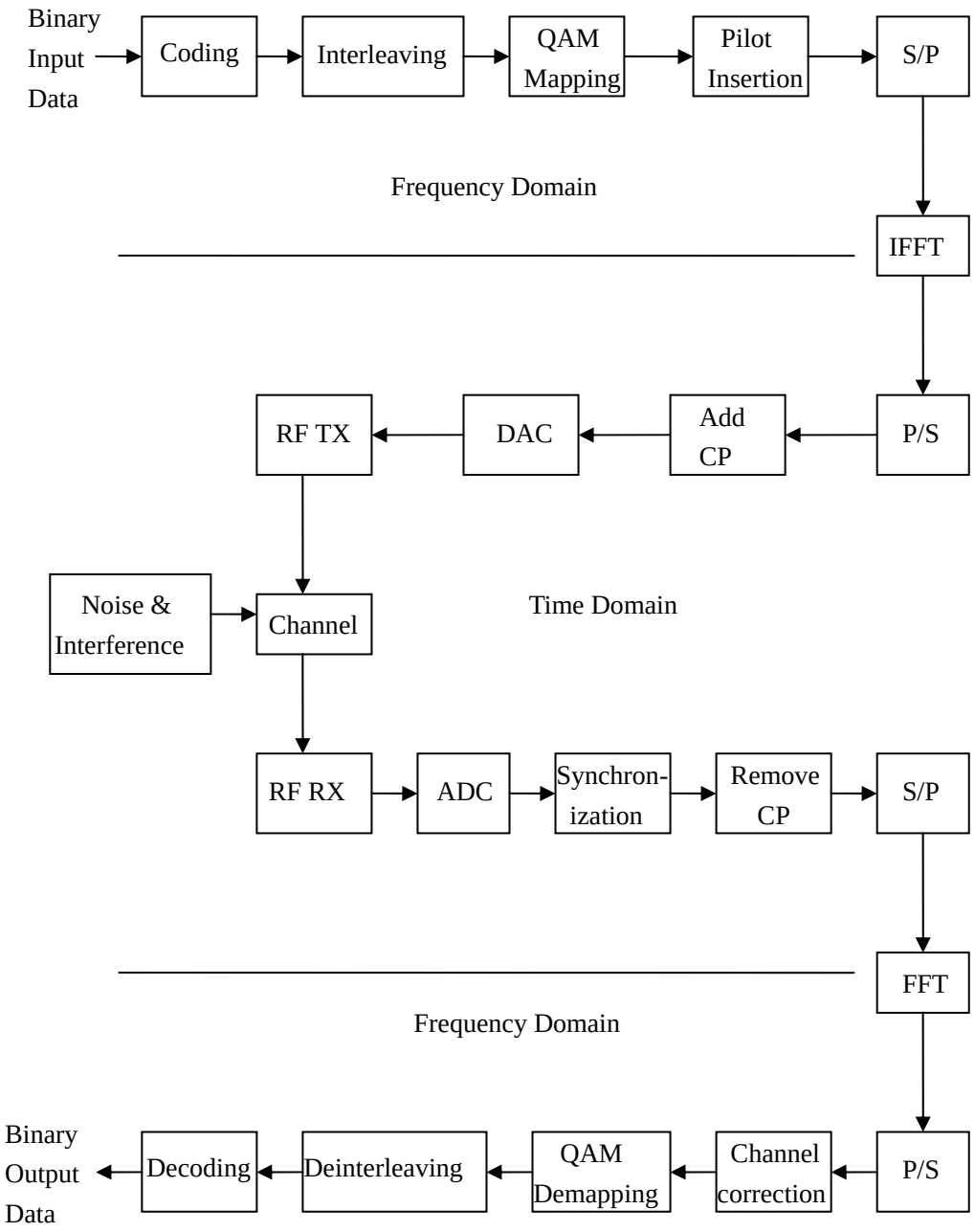

Fig. 2.2 Block diagram of an OFDM transceiver

In MC-CDMA system, each user occupies a specific subcarrier to transmit the signal, and each subcarrier is modulated by a single code chip. In other words, fractions of a MC-CDMA symbol corresponding to different chips of the spreading code are transmitted through different subcarriers [15]. In a downlink mobile radio communication channel, we can use the Hadamard Walsh codes as an optimum orthogonal set.

2.4.1 Downlink Transmitter for MC-CDMA

Fig. 2.3(a) shows the MC-CDMA transmitter for the $j-th$ user [28]. G_{MC} denotes the processing gain, N_C is the number of subcarriers, and $C^j(t) = [c_1^j\ c_2^j \ldots c_{G_{MC}}^j]$ is the spreading code for the $j-th$ user. In this figure, we assume $N_C = G_{MC}$. In fact, if the original symbol rate is high enough to be subject to frequency-selective fading, the signal needs to be converted from series to parallel (S/P) before spreading over the frequency domain. This is because for multicarrier transmission, it is essential to have frequency nonselective fading over each subcarrier [29]. In this case, the number of subcarriers can be chosen as $N_C = P \times G_{MC}$, where P is the number of the parallel sequences that the original data sequence is converted into.

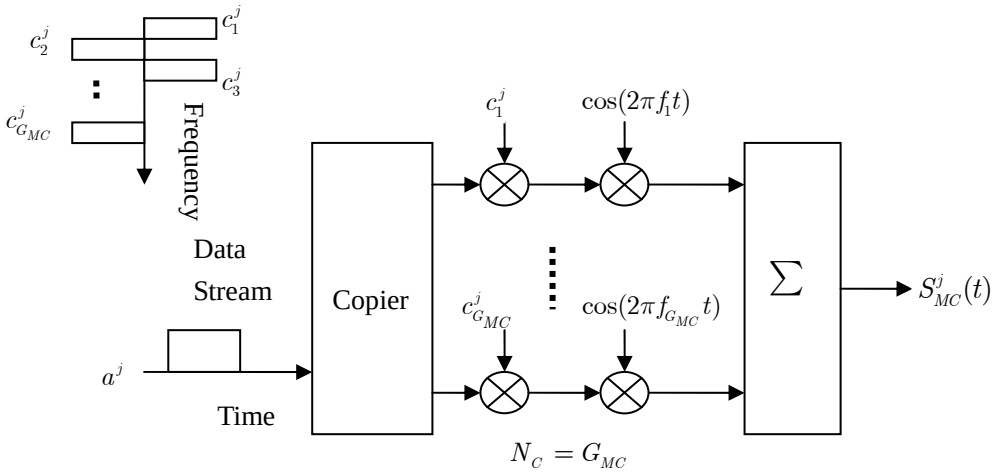

(a) Transmitter

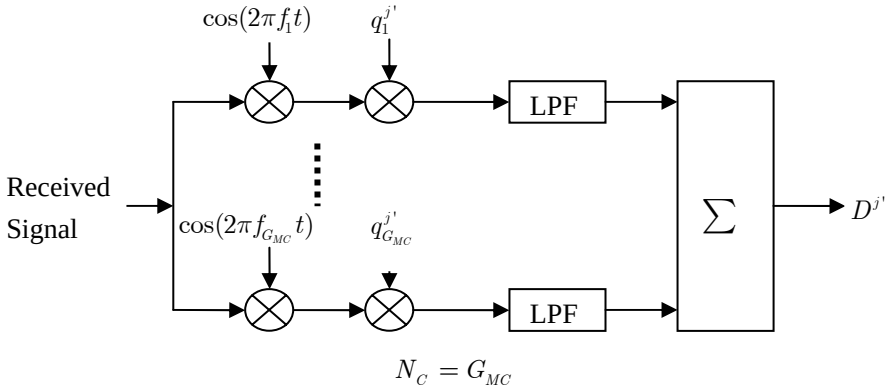

(b) Receiver

Fig. 2.3 MC-CDMA system: a) Transmitter; b) Receiver

2.4.2 Receiver for MC-CDMA

In the MC-CDMA receiver, the received signal is the summation of all the users' signals. Therefore, the receiver always employs all the received signal energy scattered in the frequency domain. However, after going through a frequency selective fading channel, all the subcarriers have different amplitude levels and different phase shifts, which result in the distortion of the orthogonality among users [28].

The MC-CDMA receiver of the $j' - th$ user is shown in Fig. 2.3(b). After the

S/P conversion, the $m-th$ subcarrier is multiplied by the gain q_m^j to combine the received signal energy which is scattered in the frequency domain. The decision variable is given by

$$D^j = \sum_{m=1}^{G_{MC}} q_m^j y_m \quad \text{with} \quad y_m = \sum_{j=1}^{J} z_m^j a^j c_m^j + n_m \tag{2.4}$$

where y_m is the complex baseband component of the received signal after down-conversion with subcarrier frequency synchronization, n_m is the additive white Gaussian noise (AWGN) at the $m-th$ subcarrier, z_m^j is the complex envelope of the $m-th$ subcarrier, a^j is the transmitted symbol for the $j-th$ user, and J is the number of active users.

2.5 Summary

Multicarrier modulation is a promising technique to meet the high data rate requirement of 4G systems. The principle of multicarrier systems is to divide the channel bandwidth into many narrowband sub-channels. The main advantages of multicarrier system are high data rate, high bandwidth efficiency, robustness against frequency selective fading and so on.

OFDM is an important type of multicarrier system. Generation of orthogonal subcarriers using IFFT is the basis of an OFDM system. Since the symbol duration increases, the relative amount of dispersion in time caused by multipath delay spread is decreased. To eliminate the inter-symbol interference, a guard interval is inserted in each OFDM symbol. Cyclic extension is used as the guard interval to avoid inter-carrier interference.

MC-CDMA, which is another important type of multicarrier system, is a combination of OFDM and CDMA. It can provide simultaneous service for a number of users. The major difference between the two types of MC systems is that MC-CDMA transmitter modulates the original signal using a given spreading code, which can be chosen from the orthogonal columns of Hadamard matrix.

Chapter 3
Estimation of Carrier Frequency Offset in Multicarrier Systems

3.1 Introduction

As mentioned in Chapter 1, the subcarriers must retain orthogonality in an OFDM system. Therefore, synchronization at the receiver is an important step that must be performed. There are at least two synchronization tasks. First, it has to find the symbol boundaries and the optimal timing instants to minimize the effects of ICI and ISI. Second, it has to estimate and compensate the carrier frequency offset to avoid ICI.

In this chapter, we present the three major causes for the loss of orthogonality briefly, as well as the compensation approaches for them. Then the sensitivity of OFDM to CFO is discussed in detail. Because of the great impairment to the OFDM performance caused by CFO, the estimation and compensation of CFO are very important in OFDM systems. As a result, a number of CFO estimation methods have been proposed in the past decade, which can be classified into two groups: data-aided and non-data-aided.

3.2 Synchronization in OFDM Systems

In an OFDM system the subcarriers cannot be perfectly orthogonal unless transmitter and receiver use exactly the same frequencies. In practice, a carrier is phase modulated by random phase jitter, leading to phase mismatch between the carriers at transmitter and receiver. As a result, the frequency, which is the time derivative of the phase, can never be perfectly constant, thereby causing ICI in an OFDM receiver [15].

3.2.1 Phase Noise

Phase noise introduces a random phase variation that is common to all subcarriers. Usually, the oscillator linewidth is much smaller than the OFDM symbol rate. Since the common phase error is strongly correlated from symbol to symbol, tracking techniques or differential detection can be used to minimize the effects of this common phase error. Another more disturbing effect of phase noise is that it destroys the orthogonality among subcarriers, which introduces ICI. The amount of ICI, which is represented by degradation in signal to noise ratio (SNR), is given by [30]

$$D \approx \frac{10}{\ln 10}\frac{11}{60}(4\pi N\frac{\beta}{R})\frac{E_s}{N_0} = \frac{11}{6\ln 10}(4\pi\beta T)\frac{E_s}{N_0} \tag{3.1}$$

where β denotes the -3dB one-sided linewidth of the power density spectrum of the carrier, E_s is the signal energy and N_0 is the AWGN power spectral density. The degradation *D* is proportional to SNR E_s/N_0 and βT, which is the ratio of the linewidth and subcarrier spacing $1/T$.

In practice, a phase-locked loop (PLL) is normally used to generate a carrier with a stable frequency. In a PLL, the frequency of a voltage-controlled oscillator (VCO) is

locked to a stable reference frequency, which is usually produced by a crystal oscillator. The PLL is able to track the phase jitter of the free-running VCO for jitter frequency components that fall within the tracking loop bandwidth. For frequencies below the tracking loop bandwidth, the phase noise of the PLL output is determined mainly by that of the reference oscillator. For frequencies larger than the tracking loop bandwidth, the phase noise is dominated by the VCO phase noise. Therefore, the PLL can lock the frequency of a VCO to a stable reference frequency [15].

3.2.2 Timing Errors

Symbol time errors are caused by an inaccurate estimate of the starting point of a symbol. There is usually some tolerance for symbol timing errors, when a cyclic prefix is used to extend the symbol [31]. If the symbol timing offset does not exceed the guard time, ICI or ISI can be avoided. Therefore, OFDM demodulation is quite insensitive to timing offsets. To achieve the best possible multipath robustness, there exists an optimal timing instant. Any deviation from that point will increase the sensitivity to delay spread. To minimize this loss of robustness, the guard interval should be designed larger than the timing error [15].

3.2.3 Frequency Offset

The OFDM subcarriers are orthogonal if each of them possesses a unique integer number of cycles within the FFT interval. However, in the presence of a frequency offset, the number of cycles in the FFT interval is not an integer anymore, which causes ICI. Each subcarrier will be interfered by all the other subcarriers. The interference power is inversely proportional to the frequency spacing [15]. An

approximation to the degradation in SNR caused by frequency offset, is given by [30]

$$D \approx \frac{10}{\ln 10}\frac{1}{3}(\pi N \frac{\triangle F}{R})^2 \frac{E_s}{N_0} = \frac{10}{3\ln 10}(\pi \triangle FT)^2 \frac{E_s}{N_0} \quad . \tag{3.2}$$

It is clear that the degradation D is proportional to the SNR and the square of the normalized frequency offset $\triangle FT$, which is the ratio of the frequency offset and the subcarrier spacing. The effect of frequency offset on the performance of OFDM system will be presented in Section 3.3 in detail.

3.3 Analysis of OFDM Systems with Carrier Frequency Offset

In the studies on the effect of CFO, the impairments are calculated in two ways. Firstly, the amount of ICI is represented by degradation in SNR or the statistical average of the carrier-to-interference ratio. Secondly, the BER could be approximated by assuming the ICI to be Gaussian [32].

In an OFDM system with frequency offset, the received signal at the $k-th$ subcarrier can be written as [30]

$$r_k = a_k I_0 + \sum_{m=0, m\neq k}^{N-1} a_m I_{m-k} + \widehat{N}_k \;\; ; \;\; k = 0,1,\ldots,(N-1) \tag{3.3}$$

where $\{a_m, m = 0,1,...,N-1\}$ are independent and equally probable QPSK symbols, and $\widehat{N}_k$ is a complex Gaussian white noise sample, the variance of which will be used to represent N_0 in the following equations. Here, the attenuation factor I_n can be written as

$$I_n = \frac{1}{T}\int_0^T e^{j2\pi\frac{n}{T}t} e^{j(2\pi f_0 t+\theta)} dt \tag{3.4}$$

where θ is the total phase, assumed to be constant over one symbol interval T, and

f_0 is frequency offset. We can also express I_n as $I_n = e^{j(\pi\varepsilon+\theta)}F_n$ where F_n is the amplitude of the interference coefficient given by

$$F_n = \mathrm{sinc}(\varepsilon)\frac{1}{1+n/\varepsilon} \tag{3.5}$$

and $\varepsilon = f_0 T$ is the normalized frequency offset. The first term on the RHS of equation (3.3) is the desired component at the $k-th$ subcarrier and is attenuated by a factor $\sin c(\varepsilon)$ and rotated by a phase $(\pi\varepsilon+\theta)$. The second term of (3.3) is an extra impairment term, known as ICI, resulting from other subcarriers due to the lack of orthogonality [33].

We define E_b as the bit energy. If ICI is assumed to be Gaussian distributed, then the average bit error probability is [34]

$$P_b = \frac{1}{2}erfc\left(\sqrt{\frac{E_b\mathrm{sinc}^2(\varepsilon)}{2(N_0/2+\sigma_{ICI}^2)}}\right) \tag{3.6}$$

where σ_{ICI}^2 is the variance of interference, i.e. the second term of (3.3). From (3.3) and (3.4), we can derive that the variance σ_{ICI}^2 will not be larger than $\frac{2}{3}\sin^2(\pi\varepsilon)E_b$. So an upper bound for the average bit error probability is given by [33]

$$P_b \le \frac{1}{2}erfc\left(\sqrt{\frac{E_b}{N_0}\cdot\frac{\mathrm{sinc}^2(\varepsilon)}{1+\frac{4}{3}\sin^2(\pi\varepsilon)E_b/N_0}}\right). \tag{3.7}$$

The degradation of SNR in dB due to the frequency offset is upper bounded by

$$\rho \le 10\log_{10}(\mathrm{sinc}^2(\varepsilon)) - 10\log_{10}(1+\frac{4}{3}\sin^2(\pi\varepsilon)E_b/N_0), \tag{3.8}$$

which is a function of ε and the SNR. In practice, the frequency offset $|\varepsilon| \ll 1$, and it is observed that this degradation is proportional to E_b/N_0, which indicates that there is an error floor on the OFDM performance. Therefore, just by increasing the

transmitted power, the error floor cannot be removed [33].

On the other hand, the lower bound for the carrier-to-interference ratio (CIR) can be expressed as [33]

$$CIR \geq \frac{3}{2(\pi\varepsilon)^2}. \tag{3.9}$$

CIR is inversely proportional to the square of the normalized frequency offset. So even a small frequency offset will reduce the CIR considerably [33].

3.4 CFO Estimation Methods

It has been shown in the preceding sections that the CFO will cause severe degradation in the performance of OFDM systems. Thus, the estimation and correction of the CFO is a very important step before the demodulation of the received signal. The two classes of the existing CFO estimators are data-aided and non-data-aided.

3.4.1 Data-aided Estimators

As its name implies, data-aided estimators commonly use pilot symbols to estimate the CFO. There are different types of pilot symbols, such as training symbols, repeated data symbols, continuous or scattered pilot symbols and so on.

A maximum likelihood based CFO estimator has been proposed in [35]. This estimator makes use of repeated data symbols, and the phase shift of the carrier between successive symbols. In the presence of small error, the estimate can be unbiased and consistent. Furthermore, this method can estimate large offset accurately because the signal values and the ICI contribute to the estimation.

Although the method in [35] gives very good performance, the repetition of the symbols uses up considerable bandwidth. To avoid this symbol repetition, an estimator using two pilot OFDM blocks has been proposed in [31]. This method avoids the extra expenses of using a null symbol, and allows larger acquisition range for the CFO. Here, the CFO estimation is implemented in two separate steps with a two-symbol training sequence. First, a training symbol, in which the first half is just the same as the second half in the time domain, is searched to find the symbol/frame timing. Then part of the CFO is corrected. The correlation of these two partially corrected training symbols is used to find the accurate estimate of CFO.

As an improvement of the above method [31], another algorithm using only one pilot block instead of two, has been proposed in [36]. This scheme also consists of two steps: tracking and acquisition. The estimation range and the variance of the estimation error is the same as the method in [31]. Because this method uses only one pilot block instead of two, its throughput efficiency is higher than that of the former.

Besides continuous pilot symbols which are used in the methods mentioned above, scattered pilots are also used in CFO estimation [37]. In OFDM systems, CFO is usually divided into an integer part and a fractional part. For this scheme, integer and coarse fractional CFO is detected by cyclic prefix in the acquisition stage. Then in the tracking stage, scattered pilots are used to detect fine fractional CFO. This method not only provides good performance but also saves the bandwidth which is used to transmit continuous pilots.

3.4.2 Non-data-aided Estimators

Although data-aided estimators have good performance, pilot symbols and training symbols occupy considerable bandwidth. As a result, the blind CFO estimation methods have received more and more attention during the past decade. There are several classes of blind estimators ([38]-[43]) which make use of null subcarriers, cyclic prefix, correlation of received signals and so on.

In [38], a joint ML estimator of time and frequency offset is proposed. This method makes use of the redundant information contained in the cyclic prefix. Because it is derived under the assumption that the channel distortion only consists of additive noise, the structure of the estimator is comparatively simple. But the simulation results show that it can also have good performance in a dispersive channel.

Another blind CFO estimator, which uses the correlation of received signals, is presented in [39]. If subcarriers are perfectly orthogonal to each other, there will be a diagonal pseudo-covariance matrix for the received signal. Therefore, a cost function is designed to enforce such a diagonal structure to find the estimate of CFO. The performance of the estimator is independent of the SNR, so it can estimate CFO accurately over low SNR. In addition, a closed-form expression is derived for the cost function to reduce the computational cost.

The intrinsic phase shift between neighbouring samples, which is due to the frequency offset, can also be used to estimate the CFO. Because this type of phase shift is independent of the subcarrier frequencies, an oversampling based deterministic CFO estimation method is proposed in [40]. The main advantage of this

method is its data efficiency — only one OFDM symbol is needed for reliable estimation.

In this thesis, we concentrate on blind estimator based on the null subcarriers concept, which does not require training pilot symbols. A polynomial cost function is constructed in [16] using null subcarriers

$$P(z) = \sum_{i=1}^{L}\sum_{k=1}^{K}\left\|\mathbf{w}_{P+i}^{H}\mathbf{Z}^{-1}\mathbf{y}(k)\right\|^{2} = \sum_{i=1}^{L}\sum_{k=1}^{K}\mathbf{w}_{P+i}^{H}\mathbf{Z}^{-1}\mathbf{y}(k)\mathbf{y}^{H}(k)\mathbf{Z}\mathbf{w}_{P+i}$$

(3.10)

where $\mathbf{w}_{P+i}$, $i = 1,\ldots,N-P$, are the columns of the IDFT matrix which modulate the null subcarriers of OFDM, $\mathbf{y}(k)$ is the receiver input for the *k*th block, and $\mathbf{Z} = diag(1, z, z^2,\ldots,z^{N-1})$ is a diagonal matrix consisting of the candidate CFO estimate ω and $z = e^{j\omega}$. The CFO estimate is the value which minimizes this cost function. In [16], the estimator searches $S \gg N$ samples for the CFO over an acquisition interval. Each search has to implement a high-cost computation with complexity of $O(2(N-1)S) + O(LKN^2)$ [41]. In order to reduce the computational complexity, Taylor's series expansion is used to replace $\mathbf{Z}^{-1}$ in [41]

$$\mathbf{Z^{-1}} = e^{-j\omega\frac{(N-1)}{2}} \times \sum_{n=0}^{+\infty}\frac{(j\omega)^n}{2^n n!}\mathbf{D}^n \qquad (3.11)$$

where $\mathbf{D} = diag((N-1),(N-3),...,(1-N))$. First several terms of (3.11) are used to construct a new approximation to the cost function (3.10), which can be written as a polynomial in the real variable ω. Then the derivative of the cost function with respect to ω is computed and set to zero. The one among the $(2Q-1)$ roots, which gives the minimum of the cost function, is the CFO estimate. By using

this rooting method instead of the search one, this estimator reduces the computational complexity significantly.

In [16] and [41], the null subcarriers are assumed to be placed at the end of the OFDM block. However, it has been proven in [42] that there may be more than one minimum for the cost function when this null subcarriers placement method is used. In order to solve the identifiability problem, three new null subcarrier insertion approaches are used in [42].

3.5 Summary

In this chapter, we discussed the performance impairment in OFDM system caused by phase noise, frequency offset and timing errors. ICI and ISI are the main causes of the degradation of the performance. Thus, synchronization at the receiver is very important. Then the sensitivity of OFDM to CFO is analyzed in detail. The amount of ICI can be represented by the degradation in SNR. Finally, two types of CFO estimation schemes are listed. Repeated symbols, pilot symbols and training symbols are usually used in data-aided estimators, while the blind schemes make use of cyclic prefix, correlation of signals, phase shift or null subcarriers to estimate the CFO.

Chapter 4

Low-cost Blind CFO Estimator for Multicarrier Systems

This chapter presents a simplified model for multicarrier system. It can be regarded as OFDM or MC-CDMA system. An existing high-cost blind CFO estimation algorithm, which makes use of null subcarriers, is summarized from the literature. Then we derive a low-cost estimator from the forenamed method. Simulation results are provided to show the performance of the proposed method compared to that of the high-cost one.

4.1 Introduction

In a practical OFDM system, not all the subcarriers are used to transmit data. Those subcarriers, named null or virtual subcarriers, are not used to avoid transmit filtering. At the transmitter, OFDM subcarriers are modulated by an IFFT matrix. By taking advantage of the orthogonality among subcarriers, a high-accuracy blind CFO estimator is proposed in [16].

In this kind of blind estimation algorithms [16] [41] [42], the location of null subcarriers is pivotal. CFO may not be determined uniquely if null subcarriers are placed consecutively [42]. Some alternatives have been proposed to resolve the identifiability problem. One is to insert the null subcarriers with distinct spacings.

Another is to make the locations of the null subcarriers different from block to block, which is called subcarrier hopping. The third method is a combination of null subcarrier hopping and consecutively located null subcarriers [42].

4.2 Simplified Model for Multicarrier System

In this section, we present a baseband model of a single-antenna multicarrier system summarized from [16] and [42]. It is shown in Fig. 4.1.

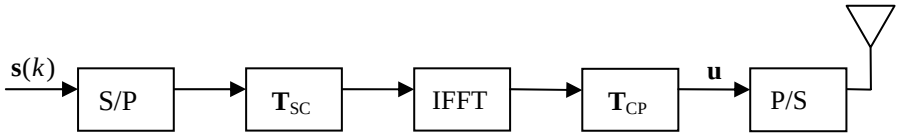

Fig. 4.1 Simplified diagram of a multicarrier system

At the transmitter, the $k-th$ block of the information stream is denoted as $\mathbf{s}(k)=[s(kK), s(kK+1),\ldots,s(kK+K-1)]^T$. After passing through the serial-to-parallel (S/P) converter, zeros are inserted in $\mathbf{s}(k)$ to obtain a vector $\mathbf{T}_{SC}\mathbf{s}(k)$ of length N. We define $\mathbf{T}_{SC} := [\mathbf{e}_{\bar{i}_1},\ldots,\mathbf{e}_{\bar{i}_K}]$ as the null subcarrier insertion matrix, where $\mathbf{e}_i$ is the $(i+1)th$ column of the $N\times N$ identity matrix $\mathbf{I}_N$. $\bar{i}_1<\cdots<\bar{i}_K$ are the indices of the information symbols, the other $i_1<\cdots<i_{N-K}$ are the indices of the inserted zeros, and $\{i_k\}_{k=1}^{N-K}\cup\{\bar{i}_k\}_{k=1}^{K}=\{0,\ldots,N-1\}$ [42]. We choose $\{\bar{i}_k\}_{k=1}^{K}=\{0,\ldots,N-K-1\}$ and $\{i_k\}_{k=1}^{N-K}=\{N-K,\ldots,N-1\}$. It means the null subcarrier insertion matrix $\mathbf{T}_{SC}=\mathbf{T}_{ZP}$, which is the zero-padding matrix [16].

After the insertion of null subcarriers, a N-point inverse FFT (IFFT) is applied to the vector $\mathbf{T}_{SC}\mathbf{s}(k)$, i.e. the symbol blocks are left multiplied with an $N\times N$ IFFT

matrix $\mathbf{F}_N^H$. Finally, a cyclic prefix (CP) is inserted in the blocks. In order to eliminate the inter-block interference (IBI), the length of the CP must not be shorter than the channel order L. Consequently, we select the length of the CP to be L, which is equal to the channel order. The final transmitted block is [42]

$$\mathbf{u}(k) = \mathbf{T}_{CP}\mathbf{F}_N^H\mathbf{T}_{SC}\mathbf{s}(k) \tag{4.1}$$

where $\mathbf{T}_{CP} = [\mathbf{I}_{L\times N}^T \ \mathbf{I}_N^T]^T$ is the CP insertion matrix. The submatrix $\mathbf{I}_{L\times N}$ consists of the last L columns of $\mathbf{I}_N$, and the length of the transmitted block is expanded to $P = N + L$. The block $\mathbf{u}(k)$ is serialized before being sent through the channel, which is assumed to be frequency-selective. The channels from transmit antenna to receive antenna have discrete-time finite impulse response $\mathbf{h} = [h(0), h(1), \ldots h(L)]$.

When the signals arrive at the receiver, they have undergone a carrier frequency offset, which could be due to Doppler or mismatch between transmit-receive oscillators, and noise corruption. We define $\omega_0 = 2\pi f_0 T$ as the normalized carrier frequency offset. The output of the filter of the receive antenna can then be written as [42]

$$x(i) = e^{j\omega_0 i}\sum_{l=0}^{L} h(l)u(i-l) + \eta(i) \tag{4.2}$$

where $\eta(i)$ is AWGN. Then the sequence $x(i)$ is S/P converted into $P\times 1$ blocks, with entries $[\mathbf{x}(k)]_p = x(kP + p)$. As the block size $P = N + L$ is greater than the channel order L in this model, the received block depends only on two consecutive transmitted blocks, which causes IBI. Since we choose L to be the length of the CP, IBI can be eliminated by left multiplying the received blocks with the CP removing matrix [42]. The IBI-free block can be written as

$$\begin{aligned}\mathbf{y}(k) &= \mathbf{R}_{CP}\mathbf{x}(k) \\ &= e^{j\omega_0 kP}\mathbf{R}_{CP}\mathbf{D}_P(\omega_0)\mathbf{H}\mathbf{T}_{CP}\mathbf{F}_N^H\mathbf{T}_{SC}\mathbf{s}(k) + \mathbf{R}_{CP}\boldsymbol{\eta}(k)\end{aligned} \tag{4.3}$$

where $\mathbf{R}_{CP} = [\mathbf{0}_{N\times L}\ \mathbf{I}_N]$ is the CP removing matrix, and the $P\times P$ diagonal matrix $\mathbf{D}_P(\omega_0)$ is defined as $\mathbf{D}_P(\omega_0) = diag[1, \exp(j\omega_0), ..., \exp(j(P-1)\omega_0)]$ which is caused by CFO ω_0. Channel matrix $\mathbf{H}$ is a $P\times P$ lower triangular Toeplitz matrix, the first column of which is $[h(0), ..., h(L), 0, ..., 0]^T$. For simplicity, we rewrite equation (4.3) as follows [44]

$$\mathbf{y}(k) = e^{j\omega_0(kP+L)}\mathbf{D}_N(\omega_0)\tilde{\mathbf{H}}\mathbf{F}_N^H\mathbf{T}_{SC}\mathbf{s}(k) + \mathbf{n}(k) \tag{4.4}$$

where $\tilde{\mathbf{H}} = \mathbf{R}_{CP}\mathbf{H}\mathbf{T}_{CP}$, $\mathbf{n}(k) = \mathbf{R}_{CP}\boldsymbol{\eta}(k)$.

In fact, the model in Fig. 4.1 can be used directly as an OFDM model. For MC-CDMA system, which is the combination of OFDM and CDMA, Fig. 4.2 shows a simple model. It is very similar to Fig. 4.1, besides the form of the vector $\mathbf{s}(k)$.

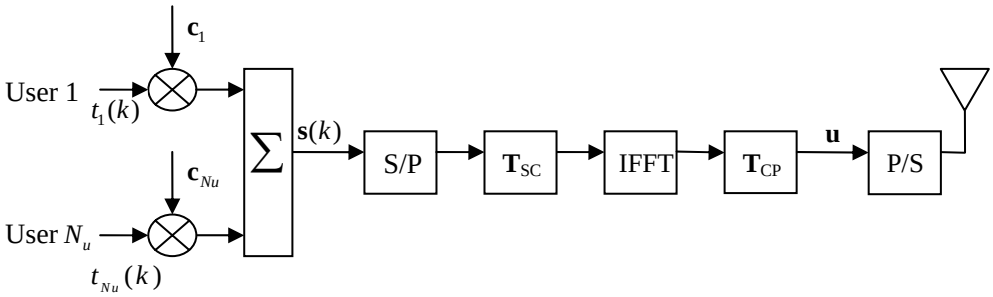

Fig. 4.2 Simple Model of Down-link MC-CDMA System

Down-link MC-CDMA system is a single-antenna multi-user system. There are N_u users in a cell. Each data bit of the $\nu - th$ user is multiplexed with a specific spreading code $\mathbf{c}_\nu = [c_\nu(0)\ c_\nu(1)\cdots c_\nu(K-1)]^T$, which is one column of orthogonal Hadamard matrix. We then sum the N_u vectors to obtain $\mathbf{s}(k)$ as

$$\mathbf{s}(k) = \sum_{\nu=1}^{N_u} t_\nu(k)\mathbf{c}_\nu \quad . \tag{4.5}$$

At user 1, which is assumed to be the user of interest, the received signal can be written as

$$\begin{aligned}\mathbf{y}(k) &= e^{j\omega_0(kP+L)}\mathbf{D}_N(\omega_0)\tilde{\mathbf{H}}\mathbf{F}_N^H\mathbf{T}_{SC}\sum_{\nu=1}^{N_u} t_\nu(k)\mathbf{c}_\nu + \mathbf{n}(k) \\ &= e^{j\omega_0(kP+L)}\mathbf{D}_N(\omega_0)\tilde{\mathbf{H}}\mathbf{F}_N^H\mathbf{T}_{SC}\mathbf{C}\mathbf{t}(k) + \mathbf{n}(k)\end{aligned} \tag{4.6}$$

where $\mathbf{C} = [\mathbf{c}_0\ \mathbf{c}_1 \ldots \mathbf{c}_{N_u}]$ is the spreading matrix and $\mathbf{t}(k) = [t_0(k)\ t_1(k) \ldots t_{N_u}(k)]^T$ is a vector which contains the $k-th$ data bits of all the users. In order to make full use of the channel, we often set $N_u = K$. If we set $\mathbf{s}(k) = \mathbf{C}\mathbf{t}(k)$, (4.6) is the same (4.4). Because every user receives not only the information sent to it, but also interferences from other users, the received signal must be recovered with the corresponding spreading code to separate the information of interest from others.

4.3 A Blind Estimator with High Computational Complexity

In this section, we present an existing blind estimation method for multicarrier system [16] [42]. The cost function is based on the received symbol and the orthogonality among the columns of the IFFT matrix.

It is known that any two columns of the IFFT matrix $\mathbf{F}_N^H$ are orthogonal to each other. So we can construct a cost function based on this as [42]

$$J(\omega) = \sum_{t=1}^{N-K} \mathbf{f}_N^H(\frac{2\pi i_t}{N})\mathbf{D}_N^{-1}(\omega)\mathbf{R}_{\mathbf{yy}}\mathbf{D}_N(\omega)\mathbf{f}_N(\frac{2\pi i_t}{N}) \tag{4.7}$$

where $\mathbf{f}_N(\frac{2\pi i}{N})$ is the $(i+1)th$ column of FFT matrix. Equation (4.7) is based on the covariance matrix $\mathbf{R}_{\mathbf{yy}}$, which is defined as $\mathbf{R}_{\mathbf{yy}} := E[\mathbf{y}(k)\mathbf{y}^H(k)]$. In practice,

$\mathbf{R}_{\mathbf{yy}}$ is estimated by averaging across *M* blocks, i.e.

$$\widehat{\mathbf{R}}_{\mathbf{yy}} = \frac{1}{M}\sum_{k=0}^{M-1}\mathbf{y}(k)\mathbf{y}^{H}(k). \tag{4.8}$$

In equation (4.7), ω is the candidate carrier offset. It has been proved in [16] that in the absence of noise, when $\omega = \omega_0$, the cost function $J(\omega_0) = 0$.

In the above sections, $\mathbf{T}_{SC} = \mathbf{T}_{ZP}$, which means that the null subcarriers are located at the end of the transmit blocks. Although this method can estimate the CFO, there is a possibility that the cost function (4.7) has non-unique global minima, which has been proved in [42]. In other words, there may be more than one CFO estimate, resulting in the so-called the identifiability problem. In this thesis, we make use of one of the proposed methods in [42], which inserts null subcarriers with distinct spacings, to resolve this problem. It has been proved that when the number of null subcarriers is $N - K = L + 2$, and the spacing between any two null subcarriers is distinct, the cost function will have a unique minimum [42]. Therefore, in the following sections, we choose the indices of the inserted zeros as $i_k = 2^{k-1}$, $k = 1,2,\ldots,N-K$, to ensure that the cost function has only one minimum.

4.4 A New Low-Cost Estimator

It is easy to get the CFO estimate by searching the candidate carrier offset ω which can minimize equation (4.7). However, this can lead to an algorithm with high computational complexity. Therefore, we develop a method with low computational cost and comparable performance.

First, we consider the inverse diagonal matrix $\mathbf{D}_N^{-1}(\omega)$, which is defined as

$$\mathbf{D}_N^{-1}(\omega) = diag(1, \exp(-j\omega), \exp(-j2\omega), ..., \exp(-j(N-1)\omega)). \tag{4.9}$$

It is known that Taylor's expansion series of a complex exponential is

$$e^{jx} = \sum_{n=0}^{+\infty} \frac{(jx)^n}{n!}. \tag{4.10}$$

Using (4.10) in (4.9), we can rewrite equation (4.9) as [41]

$$\begin{aligned}\mathbf{D}_N^{-1}(\omega) &= e^{-j\omega\frac{(N-1)}{2}} diag(e^{j\omega\frac{(N-1)}{2}}, e^{j\omega\frac{(N-3)}{2}}, \ldots, e^{j\omega\frac{(1-N)}{2}}) \\ &= e^{-j\omega\frac{(N-1)}{2}} \times \sum_{n=0}^{+\infty} \frac{(j\omega)^n}{2^n n!} \mathbf{D}^n \end{aligned} \tag{4.11}$$

where $\mathbf{D} = diag((N-1), (N-3), ..., (1-N))$. As mentioned in Chapter 1, our method is used to detect the residual CFO $|\omega_0| \ll 1$, which is less than the subcarrier spacing $\varpi = 2\pi / N$. Therefore, in the estimation, $[-\varpi \ \varpi]$ is chosen as the acquisition range. In the Taylor's series, we select a suitable integer $Q \ll N$ such that the higher order terms ($n > Q$) in (4.11) can be neglected, and the truncated series can be a good approximation to $\mathbf{D}_N^{-1}(\omega)$. The value of Q is chosen such that the absolute value of the ratio of the $(n+1)^{th}$ term to the n^{th} term of the Taylor's series of $e^{j\omega\frac{(N-1)}{2}}$ (worst case in (4.11) as the argument is the largest in absolute value) is smaller than one [41]. This results in [41]

$$Q \geq \frac{|\omega|(N-1)}{2}. \tag{4.12}$$

Now, substituting (4.8) in (4.7) leads to

$$\begin{aligned} J(\omega) &= \sum_{t=1}^{N-K} \mathbf{f}_N^H(\frac{2\pi i_t}{N}) \mathbf{D}_N^{-1}(\omega) \mathbf{R}_{\mathbf{yy}} \mathbf{D}_N(\omega) \mathbf{f}_N(\frac{2\pi i_t}{N}) \\ &\simeq \sum_{t=1}^{N-K} \mathbf{f}_N^H(\frac{2\pi i_t}{N}) \mathbf{D}_N^{-1}(\omega) \left\{ \frac{1}{M} \sum_{k=0}^{M-1} \mathbf{y}(k) \mathbf{y}^H(k) \right\} \mathbf{D}_N(\omega) \mathbf{f}_N(\frac{2\pi i_t}{N}) \\ &= \frac{1}{M} \sum_{k=0}^{M-1} \sum_{t=1}^{N-K} \left| \mathbf{f}_N^H(\frac{2\pi i_t}{N}) \mathbf{D}_N^{-1}(\omega) \mathbf{y}(k) \right|^2. \end{aligned} \tag{4.13}$$

Then, by substituting the Taylor's expansion of the inverse diagonal matrix $\mathbf{D}_N^{-1}(\omega)$ into (4.13), we can write

$$J(\omega) \approx \frac{1}{M}\sum_{k=0}^{M-1}\sum_{t=1}^{N-K}\left|\mathbf{f}_N^H(\frac{2\pi i_t}{N})\left[e^{-j\omega\frac{(N-1)}{2}}\sum_{n=0}^{+\infty}\frac{(j\omega)^n}{2^n n!}\mathbf{D}^n\right]\mathbf{y}(k)\right|^2$$

$$= \frac{1}{M}\sum_{k=0}^{M-1}\sum_{t=1}^{N-K}\left|\sum_{n=0}^{+\infty}\frac{(j\omega)^n}{2^n n!}\mathbf{f}_N^H(\frac{2\pi i_t}{N})\mathbf{D}^n\mathbf{y}(k)\right|^2 . \tag{4.14}$$

In order to simplify this equation, we set

$$a_{i_t,n}(k) = \mathbf{f}_N^H(\frac{2\pi i_t}{N})\mathbf{D}^n\mathbf{y}(k)\,. \tag{4.15}$$

Substituting (4.15) in (4.14), and replacing the infinite summations with sum over finite terms, equation (4.14) can be rewriten as

$$J_{2Q}(\omega) \approx \frac{1}{M}\sum_{k=0}^{M-1}\sum_{t=1}^{N-K}\sum_{n=0}^{Q}\sum_{m=0}^{Q}\frac{(j\omega)^n\left((j\omega)^m\right)^*}{2^{n+m}n!m!}a_{i_t,n}(k)a_{i_t,m}^*(k)$$

$$= \frac{1}{M}\sum_{k=0}^{M-1}\sum_{n=0}^{Q}\sum_{m=0}^{Q}\frac{(-1)^m(j\omega)^{n+m}}{2^{n+m}n!m!}\sum_{t=1}^{N-K}a_{i_t,n}(k)a_{i_t,m}^*(k)\,. \tag{4.16}$$

It is obvious that $J(\omega) = \lim_{Q\to\infty} J_{2Q}(\omega)$. For simplicity, we can rewrite the previous equation as follows

$$J_{2Q}(\omega)$$

$$\approx \sum_{l=0}^{2Q}(\frac{j}{2})^l\omega^l\sum_{m=0}^{l}\frac{(-1)^m}{(l-m)!m!}\sum_{t=1}^{N-K}\left\{\frac{1}{M}\sum_{k=0}^{M-1}a_{i_t,l-m}(k)a_{i_t,m}^*(k)\right\}$$

$$= \sum_{l=0}^{2Q}p_l\omega^l \tag{4.17}$$

where the polynomial coefficients p_l are given by

$$p_l = (\frac{j}{2})^l\sum_{m=0}^{l}\frac{(-1)^m}{(l-m)!m!}\sum_{t=1}^{N-K}\left\{\frac{1}{M}\sum_{k=0}^{M-1}a_{i_t,l-m}(k)a_{i_t,m}^*(k)\right\} \tag{4.18}$$

keeping in mind that $a_{i,l}(k) = 0$ if $l > Q$.

From (4.17) we can see that $J_{2Q}(\omega)$ is a polynomial of the real variable ω of

degree 2*Q*, and the polynomial coefficients p_l have been proven to be real in [41]. Hence, the value ω which can minimize (4.17) is the CFO estimate. Because equation (4.17) is a polynomial of the variable ω, we can estimate the CFO by computing its derivative with respect to ω and setting it to zero. The derivative is

$$\frac{\partial J_{2Q}(\omega)}{\partial \omega} = \sum_{l=1}^{2Q} l p_l \omega^{l-1} = 0 . \tag{4.19}$$

In general, there will be up to (2*Q*-1) roots. The estimated carrier offset $\hat{\omega}_0$ is the one, which once substituted in (4.17), gives the minimum of the cost function.

Besides the rooting method, there is another way to compute the CFO estimate. We can evaluate equation (4.17) for different values of the angle ω over an interval of interest. The estimated carrier offset $\hat{\omega}_0$ will be the value of ω for which $J_{2Q}(\omega)$ is minimum. This search method is the same as the one we use to find the minimum of equation (4.7).

4.5 Simulation Results

In this part, we present the numerical results of the low-cost method. The method is applied to two types of multicarrier systems: OFDM and MC-CDMA. The performance of the high-cost method and the proposed method is compared. In all simulations, we use QPSK modulation. The transmitted signal is corrupted with AWGN. The definition of SNR is $SNR = E_s / \sigma_\eta^2$, where E_s is the energy per symbol and σ_η^2, the variance of AWGN $\eta(i)$, is used to represent the noise power spectral density $N_0 = \sigma_\eta^2$. The mean square error (MSE) is defined as

$$MSE = \frac{1}{N_S}\sum_{i=1}^{N_S}(\frac{\hat{\omega}_0 - \omega_0}{\varpi})^2 \quad . \tag{4.20}$$

where $\varpi = 2\pi / N$ is the subcarrier spacing. The MSE is computed using $N_S = 300$ Monte Carlo trials.

4.5.1 Simulation Results for OFDM System

Firstly, we show the performance of the proposed method under the same conditions that is used in Fig. 4 [42] (*L*=1, *K*=13, *N*=16 and $\mathbf{h} = [1/\sqrt{2},\ j/\sqrt{2}]^T$). In Fig. 4.3, we present the CFO estimates for *Q*=1 and *Q*=2 when $\omega_0 = 0.01\pi$. We find that when *Q*=2, the result of having distinct-spacing is very close to the result of Ma et al [42]. And it is much better than the results of the consecutive null subcarriers, which is consistent to the conclusion of [42].

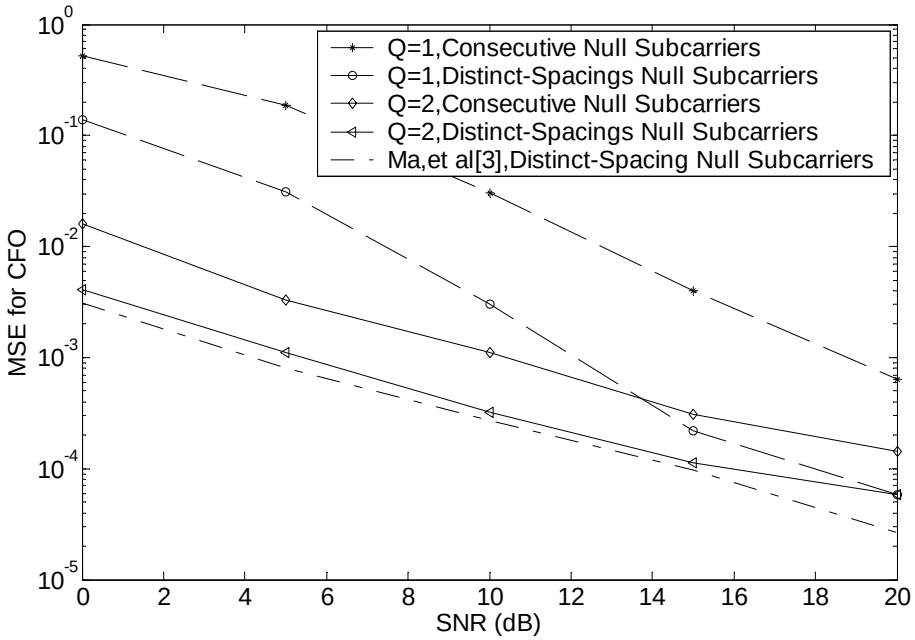

Fig. 4.3 MSE of CFO estimation for OFDM using both the proposed and Ma et al [42] methods, *Q*=1 & *Q*=2 and $\omega_0 = 0.01\pi$

In the following figures, the CFO is $\omega_0 = 0.1\varpi$. The channel between transmitter and receiver is Rayleigh fading. We assume that the channel order is $L = 3$ and

choose $N = 32$ (the number of symbols in each transmitted block after null subcarrier insertion). As we mentioned earlier, the null subcarriers are inserted into the blocks with distinct spacing. The subcarrier spacing is $\varpi = 2\pi / N$. The estimated correlation matrix $\hat{\mathbf{R}}_{yy}$ is averaged over M=320 blocks.

Fig. 4.4 compares the performance of the proposed method with the high-cost one. When $Q = 1$, the performance at low SNR is not good. It is because that the truncation error is too large. But the result for $Q = 2$ is comparable. When $Q = 3$, the performance of proposed method is almost as good as the former one.

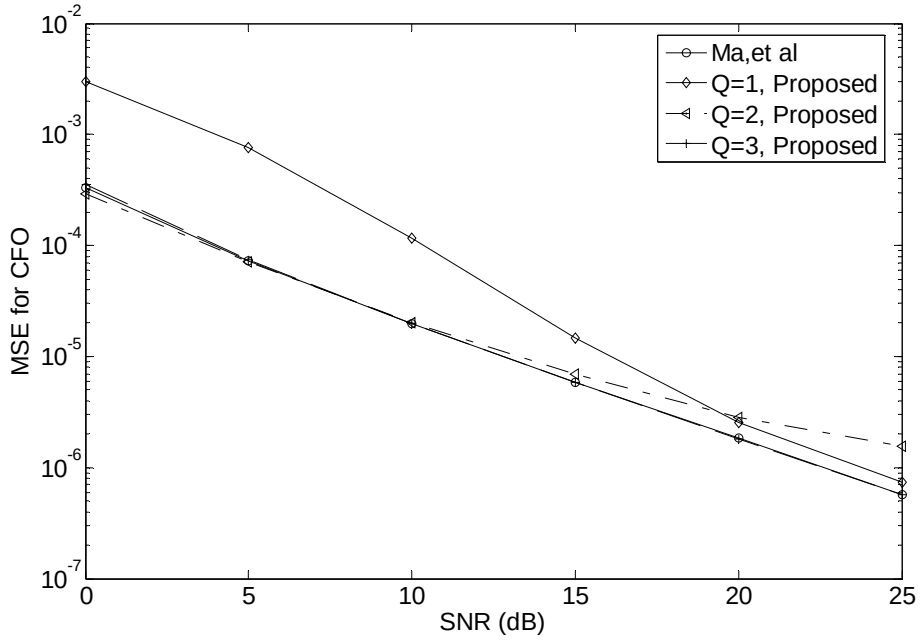

Fig. 4.4 MSE of CFO estimation for OFDM system using both the proposed and Ma et al [42] methods, $\omega_0 = 0.1\varpi$

In Fig. 4.5, we choose different number of blocks M, across which the estimated correlation matrix $\hat{\mathbf{R}}_{yy}$ is averaged. The value of M is taken as N, $5N$ and $10N$ for the cases considered here. The performance improves with M. The reason is that the covariance matrix can be estimated more accurately when the

number of averaged blocks is greater.

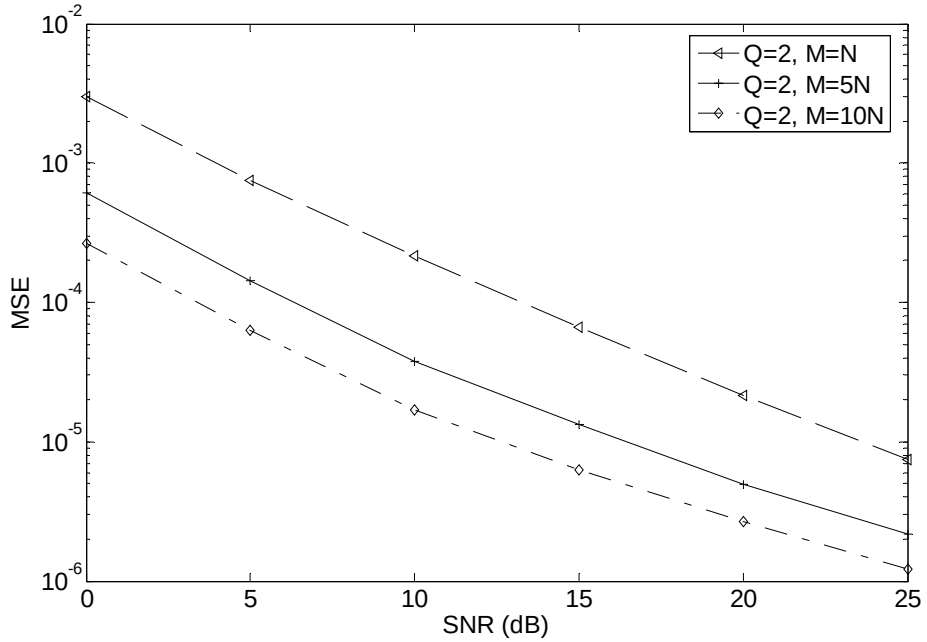

Fig. 4.5 MSE of CFO estimation for OFDM system using the proposed method, $Q = 2$, $\omega_0 = 0.1\varpi$

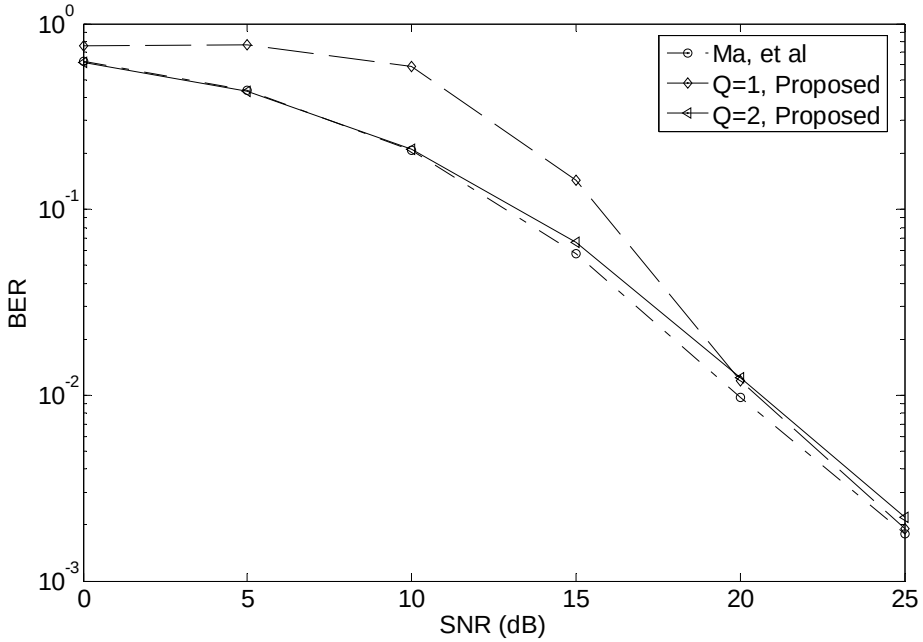

Fig. 4.6 BER of OFDM system using both the proposed and Ma et al [42] methods, $Q = 1$, $Q = 2$, $\omega_0 = 0.1\varpi$

Fig. 4.6 shows the bit error rate (BER) of OFDM systems. The proposed method gives comparable results with $Q = 2$ as compared to the high-cost one.

4.5.2 Simulation Results for MC-CDMA System

In MC-CDMA system we select $K = 24$, because K is also the order of the Hadamard matrix, for which *K* must be an integer and *K*, *K/12* or *K/20* must be a power of 2. So there will be 8 null subcarriers in one block. But we also insert $L + 2 = 5$ null subcarriers into the information blocks, and the other 3 null subcarriers are located at the end of the blocks. When we construct the cost function, only $L + 2$ distinct-spacing null subcarriers are included.

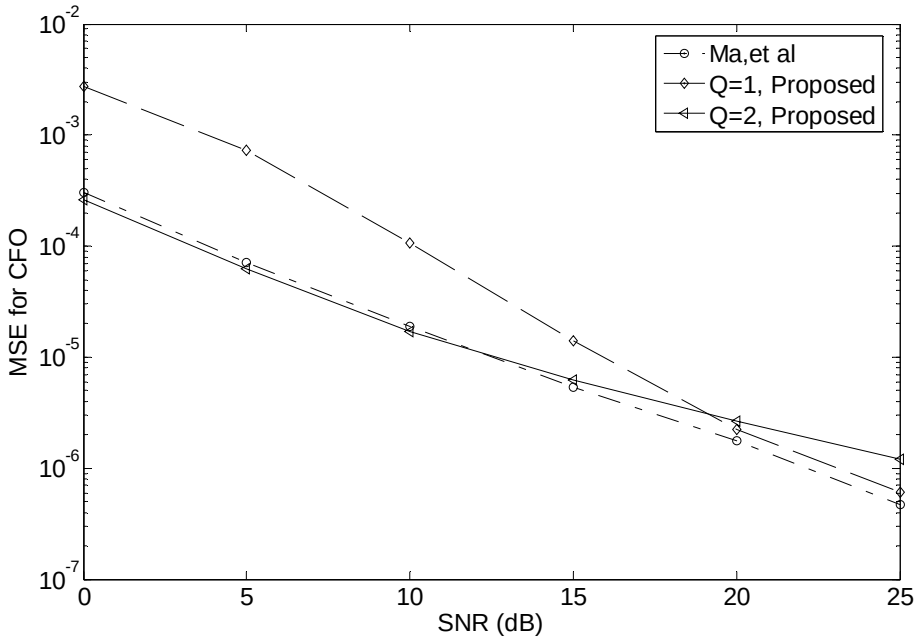

Fig. 4.7 MSE of CFO estimation for MC-CDMA system using both the proposed and Ma et al [42] methods, $\omega_0 = 0.1\varpi$

Fig. 4.7 shows the performance of the proposed method and the high-cost method. Similar to OFDM system, the truncation error of the proposed method with $Q=1$ is large. But when $Q=2$, the result of the low-cost method is comparable with the high-cost one.

Figs. 4.8 and 4.9 show the results when the CFO ω_0 is varied uniformly over the interval $[-0.125\varpi \ 0.125\varpi]$ and $[-0.25\varpi \ 0.25\varpi]$. Observe that when $\omega_0 \in [-0.125\varpi \ 0.125\varpi]$, the proposed method with $Q=2$ can give comparable results. But when $\omega_0 \in [-0.25\varpi \ 0.25\varpi]$, the performance with $Q=2$ is not good enough because of the big truncation error. We need to choose $Q=3$ to get better results. It is clear that the larger the CFO, the more terms of the Taylor's series are needed for estimation.

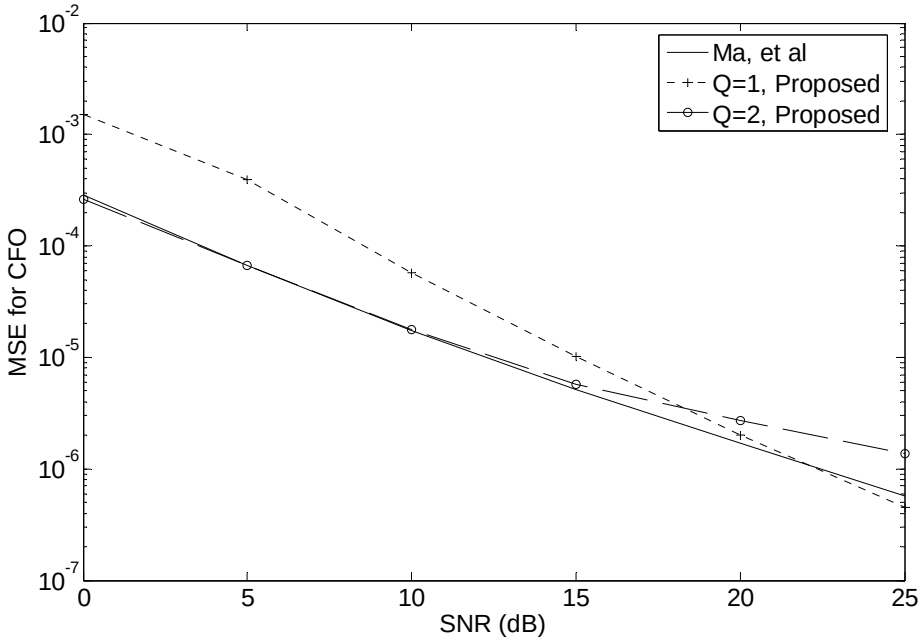

Fig. 4.8 MSE of CFO estimation for MC-CDMA system using both the proposed and Ma et al [42] methods, $\omega_0 \in [-0.125\varpi \ \ 0.125\varpi]$

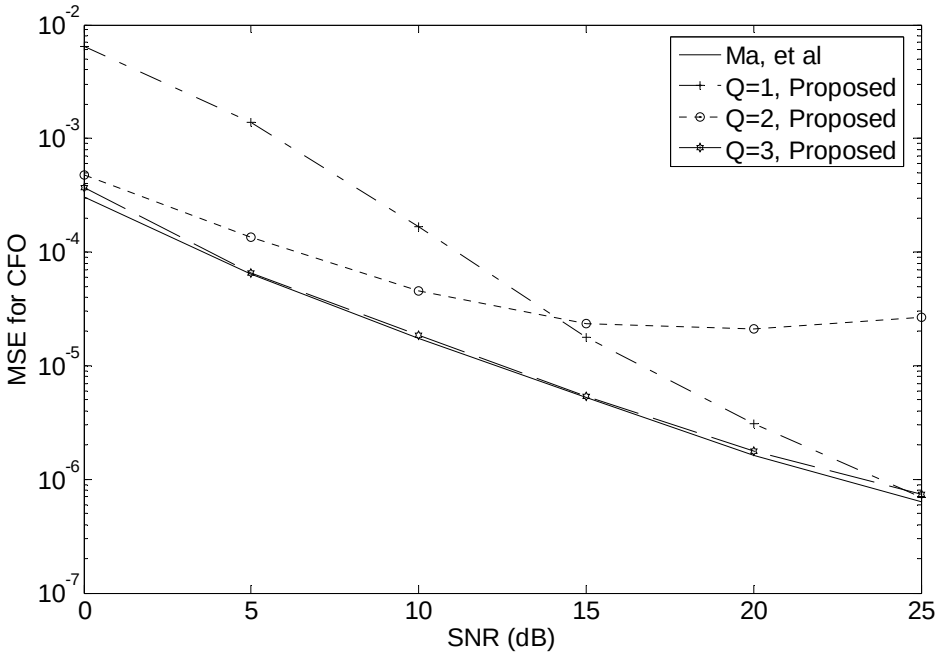

Fig. 4.9 MSE of CFO estimation for MC-CDMA system using both the proposed and Ma et al [42] methods, $\omega_0 \in [-0.25\varpi \quad 0.25\varpi]$

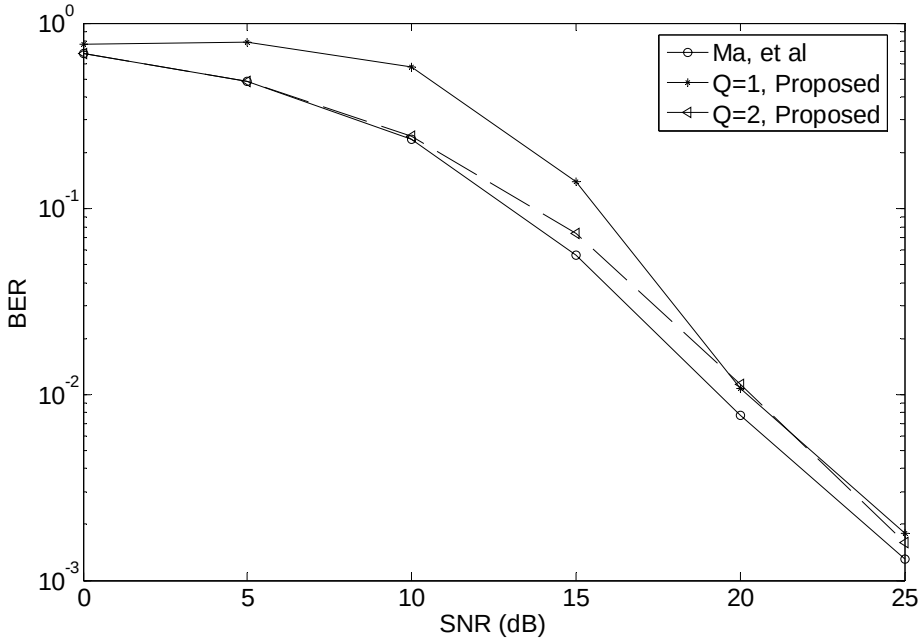

Fig. 4.10 BER of MC-CDMA system using both the proposed and Ma et al [42] methods, $\omega_0 = 0.1\varpi$

Fig. 4.10 presents the BER of MC-CDMA system. As in Fig. 4.8, when $Q=2$, the performance is good.

From Figs.4.4, 4.7, 4.8 and 4.9, we can find that when SNR is low, the result for $Q=2$ is better than that for $Q=1$. But the performance for $Q=1$ is better than that for $Q=2$ at high SNR. In fact, with increase in SNR, there are boundaries for these two cases (a figure will be provided in next chapter). These phenomena do not appear in the results for $Q=3$ and $Q=4$. As a result, when SNR is high, we must choose $Q\geq 3$ to estimate the CFO. These problems exist not only in SISO systems, but also in the MIMO systems. We will try to explain the reason for this in the next chapter.

4.6 Summary

In this chapter, a low-cost blind method is presented to estimate carrier frequency offset for multi-carrier systems. The algorithm not only gives good performance, but also ensures the uniqueness of the CFO estimate. Taylor's series expansion is used to reduce the computational cost, which will be discussed in detail in the next chapter.

In the simulation section, we presented two cases of multicarrier systems: OFDM and MC-CDMA. The results of these two specific cases show that the performance of the low-cost method is comparable with the high-cost one. And we also found that when the CFO ω_0 increases, the parameter Q must be increased to ensure the accuracy of the estimator. This problem will also be presented in the next chapter.

Chapter 5

Low-cost Blind CFO Estimator for MIMO Multicarrier Systems

It has been shown in the previous chapter that the proposed estimation method gives good performance in multicarrier systems. In this chapter, we extend the method to multi-input multi-output (MIMO) multicarrier systems. We will discuss how the new method reduces the computational cost in detail, and the relationship between the CFO ω_0 and parameter Q.

5.1 Introduction

Multiple antennas have been applied in wireless communications for a long time. The main effect is to reduce the interference between co-channel signals or users. When there is a strong line of sight (LOS) connection between the transmitter and receiver, multiple antennas are usually used to exploit the channel resources.

As the combination of MIMO and multicarrier techniques, MIMO multicarrier system offers high data rate, high bandwidth efficiency, robustness to frequency-selective fading and so on. So the MIMO multicarrier system is considered a promising technique for high speed wireless communication in the future. As with any multicarrier system, the MIMO multicarrier system is also sensitive to carrier

frequency offset. The estimators, which are used for multicarrier system, can also be extended to MIMO multicarrier system.

5.2 MIMO Multicarrier System Model

First, we present a general model of MIMO multi-carrier system based on [44] [47], which is shown in Fig. 5.1. This is a simplified down-link model based on the following assumptions:

• All the users' signals, which are transmitted from a specific transmit antenna to specific receive antenna, are propagated through the same channel.

• All the signals received at the user of interest are interfered by the same carrier frequency offsets, because they are frequency shifted using the same oscillator at the transmitter.

We assume that there are N_u users randomly distributed in a cell site. The number of transmit and receive antennas are N_t and N_r, respectively. At the transmitter, the information of the $\nu - th$ user is space-division multiplexed to yield N_t data streams $\left\{\mathbf{t}_\mu^\nu(k)\right\}_{\mu=1}^{N_t}$. After passing through the S/P converter, $\mathbf{t}_\mu^\nu(k)$ is converted into a parallel set of symbols $\{t_\mu^\nu(q)\}_{q=0}^{K-1}$. Then each symbol is multiplied by $c_\mu^\nu(q)$, which is one element of the spreading sequence $\mathbf{c}_\mu^\nu = [c_\mu^\nu(0)\ c_\mu^\nu(1)\cdots c_\mu^\nu(K-1)]^T$. The output of the coder can be written as $\tilde{\mathbf{s}}_\mu^\nu(k) = [t_\mu^\nu(0)c_\mu^\nu(0)\ \ t_\mu^\nu(1)c_\mu^\nu(1)\ \ \ldots t_\mu^\nu(K-1)c_\mu^\nu(K-1)\ ]^T$.

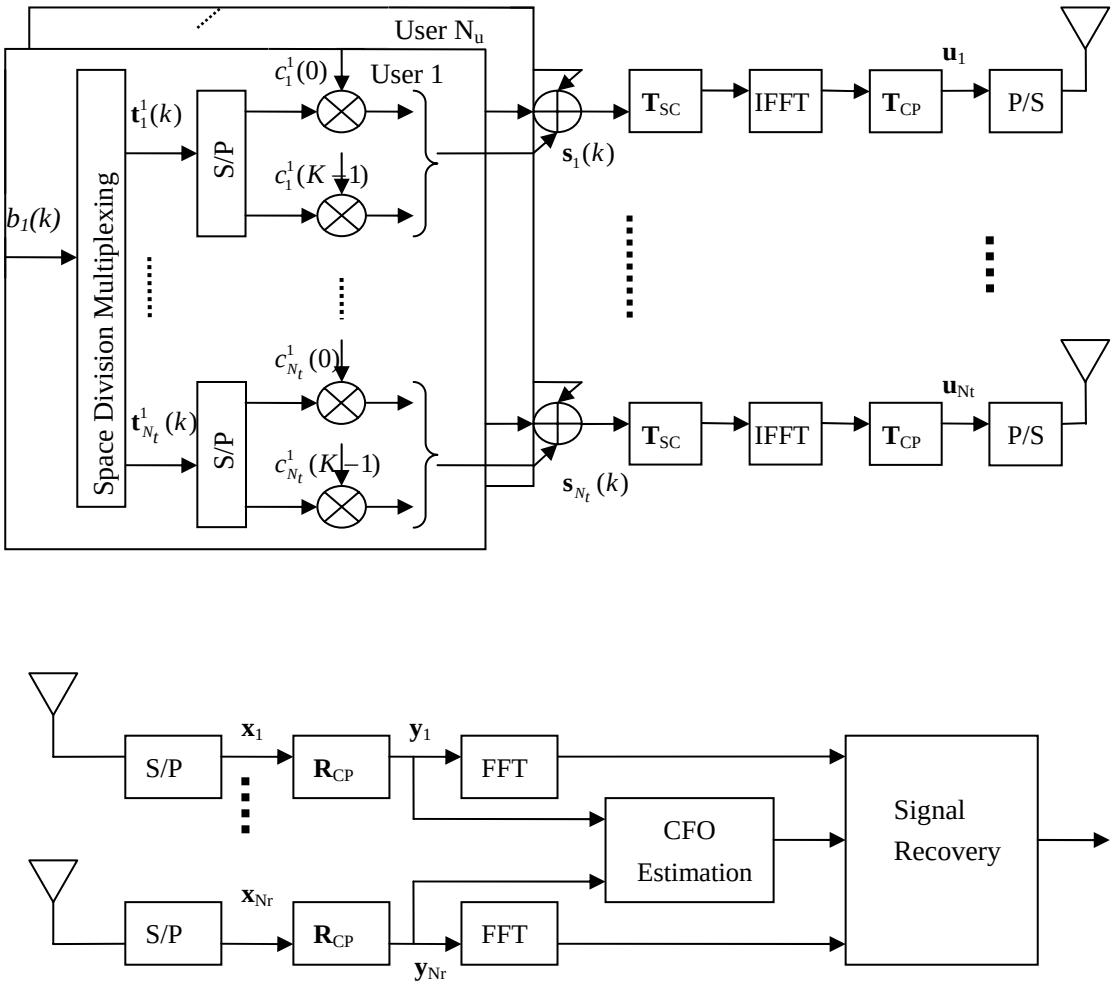

Fig. 5.1 General model for down-link MIMO multicarrier system:
Transmitter and Receiver

All the N_u vectors corresponding to the $\mu - th$ antenna are summed together to yield the vector:

$$\mathbf{s}_\mu(k) = \sum_{\nu=1}^{N_u} \tilde{\mathbf{s}}_\mu^\nu(k) \tag{5.1}$$

where the vectors $\{\mathbf{s}_\mu(k)\}_{\mu=1}^{N_t}$ are of length K. Then, we just perform OFDM to $\mathbf{s}_\mu(k)$ as [44]. We add null subcarriers (via left multiplication with $\mathbf{T}_{SC}$), implement IFFT (via left multiplication with $\mathbf{F}_N^H$) and insert cyclic prefix (via left multiplication

with $\mathbf{T}_{CP}$). The final transmitted block of the $\mu - th$ antenna can be written as

$$\mathbf{u}_{\mu}(k) = \mathbf{T}_{CP}\mathbf{F}_N^H\mathbf{T}_{SC}\mathbf{s}_{\mu}(k). \tag{5.2}$$

The blocks $\{\mathbf{u}_{\mu}(k)\}_{\mu=1}^{N_t}$ are transmitted through frequency-selective channels. The channels from $\mu - th$ transmit antenna to $\upsilon - th$ receive antenna have discrete-time finite impulse responses $h^{(\upsilon,\mu)}(l), l \in [0, L]$. When the signals arrive at the receiver, they have undergone a carrier frequency offset ω_0.

Let us consider one of the N_r receive antennas. The output of the filter of the $\upsilon - th$ receive antenna can be written as [44]

$$x_{\upsilon}(i) = e^{j\omega_0 i}\sum_{\mu=1}^{N_t}\sum_{l=0}^{L} h^{(\upsilon,\mu)}(l)u_{\mu}(i-l) + \eta_{\upsilon}(i) \tag{5.3}$$

where $\upsilon \in \{1,2,\ldots,N_r\}$, and $\eta_{\upsilon}(i)$ is additive white Gaussian noise. We can show that every antenna receives the sum of the signals coming from the N_t transmit antennas. Recall from Chapter 4, IBI can be eliminated by left multiplying received blocks with the CP removing matrix [42]. Then the IBI-free block can be written as

$$\begin{aligned}\mathbf{y}_{\upsilon}(k) &= \mathbf{R}_{CP}\mathbf{x}_{\upsilon}(k) \\ &= e^{j\omega_0 kP}\sum_{\mu=1}^{N_t}\mathbf{R}_{CP}\mathbf{D}_P(\omega_0)\mathbf{H}^{(\upsilon,\mu)}\mathbf{T}_{CP}\mathbf{F}_N^H\mathbf{T}_{SC}\mathbf{s}_{\mu}(k) + \mathbf{R}_{CP}\boldsymbol{\eta}_{\upsilon}(k)\end{aligned} \tag{5.4}$$

where channel matrix $\mathbf{H}^{(\upsilon,\mu)}$ is a $P \times P$ lower triangular Toeplitz matrix, the first column of which is $[h^{(\upsilon,\mu)}(0),\ldots,h^{(\upsilon,\mu)}(L),0,\ldots,0]^T$. For simplicity, we rewrite equation (5.4) as follows [44]

$$\mathbf{y}_{\upsilon}(k) = e^{j\omega_0(kP+L)}\mathbf{D}_N(\omega_0)\sum_{\mu=1}^{N_t}\tilde{\mathbf{H}}^{(\upsilon,\mu)}\mathbf{F}_N^H\mathbf{T}_{SC}\mathbf{s}_{\mu}(k) + \mathbf{n}_{\upsilon}(k) \tag{5.5}$$

where $\tilde{\mathbf{H}}^{(\upsilon,\mu)} = \mathbf{R}_{CP}\mathbf{H}^{(\upsilon,\mu)}\mathbf{T}_{CP}$ and $\mathbf{n}_{\upsilon}(k) = \mathbf{R}_{CP}\boldsymbol{\eta}_{\upsilon}(k)$.

5.3 Blind CFO Estimator

The cost function of the high-cost estimation algorithm for MIMO multicarrier system is as that given in (4.7). But the definition of the covariance matrix is different. In MIMO multicarrier system, the covariance matrix $\mathbf{R}_{\mathbf{yy}}$ is the summation of the covariance matrices $\mathbf{R}_{\mathbf{y}_v}$ of $\{\mathbf{y}_v(k)\}_{v=1}^{N_r}$. We define $\mathbf{R}_{\mathbf{y}_v} = E[\mathbf{y}_v(k)\mathbf{y}_v^H(k)]$. In practice, $\mathbf{R}_{\mathbf{y}_v}$ is estimated by averaging across *M* blocks, i.e.

$$\widehat{\mathbf{R}}_{\mathbf{y}_v} = \frac{1}{M}\sum_{k=0}^{M-1}\mathbf{y}_v(k)\mathbf{y}_v^H(k). \tag{5.6}$$

So the covariance matrix $\mathbf{R}_{\mathbf{yy}}$ can be written as

$$\mathbf{R}_{\mathbf{yy}} \simeq \sum_{v=1}^{N_r}\widehat{\mathbf{R}}_{\mathbf{y}_v} = \frac{1}{M}\sum_{v=1}^{N_r}\sum_{k=0}^{M-1}\mathbf{y}_v(k)\mathbf{y}_v^H(k). \tag{5.7}$$

Substituting (5.7) in the cost function in (4.7), the equation can be rewritten as

$$\begin{aligned} J(\omega) &= \sum_{t=1}^{N-K}\mathbf{f}_N^H(\frac{2\pi i_t}{N})\mathbf{D}_N^{-1}(\omega)\left\{\sum_{v=1}^{N_r}\mathbf{R}_{\mathbf{y}_v}\right\}\mathbf{D}_N(\omega)\mathbf{f}_N(\frac{2\pi i_t}{N}) \\ &\simeq \sum_{t=1}^{N-K}\mathbf{f}_N^H(\frac{2\pi i_t}{N})\mathbf{D}_N^{-1}(\omega)\left\{\sum_{v=1}^{N_r}\left[\frac{1}{M}\sum_{k=0}^{M-1}\mathbf{y}_v(k)\mathbf{y}_v^H(k)\right]\right\}\mathbf{D}_N(\omega)\mathbf{f}_N(\frac{2\pi i_t}{N}) \\ &= \frac{1}{M}\sum_{v=1}^{N_r}\sum_{k=0}^{M-1}\sum_{t=1}^{N-K}\left|\mathbf{f}_N^H(\frac{2\pi i_t}{N})\mathbf{D}_N^{-1}(\omega)\mathbf{y}_v(k)\right|^2. \end{aligned} \tag{5.8}$$

By substituting Taylor's expansion of the inverse diagonal matrix $\mathbf{D}_N^{-1}(\omega)$ in (5.8), we can write

$$\begin{aligned} J(\omega) &\approx \frac{1}{M}\sum_{v=1}^{N_r}\sum_{k=0}^{M-1}\sum_{t=1}^{N-K}\left|\mathbf{f}_N^H(\frac{2\pi i_t}{N})\left[e^{-j\omega\frac{(N-1)}{2}}\sum_{n=0}^{+\infty}\frac{(j\omega)^n}{2^n n!}\mathbf{D}^n\right]\mathbf{y}_v(k)\right|^2 \\ &= \frac{1}{M}\sum_{v=1}^{N_r}\sum_{k=0}^{M-1}\sum_{t=1}^{N-K}\left|\sum_{n=0}^{+\infty}\frac{(j\omega)^n}{2^n n!}\mathbf{f}_N^H(\frac{2\pi i_t}{N})\mathbf{D}^n\mathbf{y}_v(k)\right|^2. \end{aligned} \tag{5.9}$$

In order to simplify this equation, we set

$$a_{i_t,n}^{v}(k) = \mathbf{f}_N^H(\frac{2\pi i_t}{N})\mathbf{D}^n\mathbf{y}_v(k). \tag{5.10}$$

Substituting (5.10) into (5.9), and replacing the infinite summations with finite ones, equation (5.9) can be rewrite as

$$J_{2Q}(\omega) \approx \frac{1}{M}\sum_{v=1}^{N_r}\sum_{k=0}^{M}\sum_{t=1}^{N-K}\sum_{n=0}^{Q}\sum_{m=0}^{Q}\frac{(j\omega)^n\left((j\omega)^m\right)^*}{2^{n+m}n!m!}a_{i_t,n}^{v}(k)\left(a_{i_t,m}^{v}(k)\right)^*$$

$$= \frac{1}{M}\sum_{v=1}^{N_r}\sum_{k=0}^{M}\sum_{n=0}^{Q}\sum_{m=0}^{Q}\frac{(-1)^m(j\omega)^{n+m}}{2^{n+m}n!m!}\sum_{k=1}^{N-K}a_{i_t,n}^{v}(k)\left(a_{i_t,m}^{v}(k)\right)^* . \tag{5.11}$$

It is obvious that $J(\omega) = \lim_{Q\to\infty} J_{2Q}(\omega)$. For simplicity, we can rewrite the previous equation as follows

$$J_{2Q}(\omega)$$

$$\approx \sum_{l=0}^{2Q}(\frac{j}{2})^l\omega^l\sum_{m=0}^{l}\frac{(-1)^m}{(l-m)!m!}\sum_{t=1}^{N-K}\left\{\frac{1}{M}\sum_{v=1}^{N_r}\sum_{k=0}^{M}a_{i_t,l-m}^{v}(k)\left(a_{i_t,m}^{v}(k)\right)^*\right\}$$

$$= \sum_{l=0}^{2Q}p_l\omega^l \tag{5.12}$$

where the polynomial coefficients p_l are given by

$$p_l = (\frac{j}{2})^l\sum_{m=0}^{l}\frac{(-1)^m}{(l-m)!m!}\sum_{t=1}^{N-K}\left\{\frac{1}{M}\sum_{v=1}^{N_r}\sum_{k=0}^{M}a_{i_t,l-m}^{v}(k)\left(a_{i_t,m}^{v}(k)\right)^*\right\} \tag{5.13}$$

keeping in mind that $a_{i,l}(k) = 0$ if $l > Q$.

Then we can use the frequency rooting method or search method in Chapter 4 to estimate the carrier offset $\hat{\omega}_0$.

5.4 Performance Analysis

In this section, we analyze the perturbation, which is caused by additive white Gaussian noise, to the performance of the proposed estimator. The measure of the performance is the theoretical MSE of the CFO estimate. A closed-form function is derived to reveal the relation between system parameters and the performance of the

estimator. Since the MSE of the proposed method varies with the value of Q, we make use of the cost function (5.8) to derive a deterministic theoretical MSE to benchmark the results of the low-cost estimation algorithm.

First, we write the received block (5.5) as $\mathbf{y}_v(k) = \tilde{\mathbf{y}}_v(k) + \mathbf{n}_v(k)$, where $\tilde{\mathbf{y}}_v(k)$ is the information part and $\mathbf{n}_v(k)$ is the perturbation part， which is assumed to be independent and identically distributed (i.i.d.) circular complex-valued additive noise of zero-mean. An expression of the perturbation in the CFO estimates has been derived in [46]

$$\Delta\omega = -\frac{\left.\frac{\partial J(\omega)}{\partial \omega}\right|_{\omega=\omega_0}}{\left.\frac{\partial^2 J(\omega)}{\partial \omega^2}\right|_{\omega=\omega_0}} \tag{5.14}$$

where $\Delta\omega = \hat{\omega}_0 - \omega_0$.

Based on the knowledge that

$$\begin{cases} \mathbf{y}_v(k)\mathbf{y}_v^H(k) = \tilde{\mathbf{y}}_v(k)\tilde{\mathbf{y}}_v^H(k) + \tilde{\mathbf{y}}_v(k)\mathbf{n}_v^H(k) + \mathbf{n}_v(k)\tilde{\mathbf{y}}_v^H(k) + \mathbf{n}_v(k)\mathbf{n}_v^H(k) \\ \mathbf{f}_N^H\left(\frac{2\pi i_t}{N}\right)\mathbf{D}_N^{-1}(\omega_0)\tilde{\mathbf{y}}_v(k) = \tilde{\mathbf{y}}_v^H(k)\mathbf{D}_N(\omega_0)\mathbf{f}_N\left(\frac{2\pi i_t}{N}\right) = 0 \end{cases}, \tag{5.15}$$

we can obtain the numerator of (5.14) by performing first-order derivative to the cost function (5.8), which can be expressed as [46]

$$\begin{aligned} &\left.\frac{\partial J(\omega)}{\partial \omega}\right|_{\omega=\omega_0} \\ &= -\frac{j}{M}\left\{\sum_{v=1}^{N_r}\sum_{k=0}^{M-1}\sum_{t=1}^{N-K}\left(\mathbf{f}_N^H\left(\frac{2\pi i_t}{N}\right)\mathbf{D}_N^{-1}(\omega_0)\tilde{\mathbf{D}}_N\tilde{\mathbf{y}}_v(k)\mathbf{n}_v^H(k)\mathbf{D}_N(\omega_0)\mathbf{f}_N\left(\frac{2\pi i_t}{N}\right)\right)\right\} \\ &\quad + \frac{j}{M}\left\{\sum_{v=1}^{N_r}\sum_{k=0}^{M-1}\sum_{t=1}^{N-K}\left(\mathbf{f}_N^H\left(\frac{2\pi i_t}{N}\right)\mathbf{D}_N^{-1}(\omega_0)\mathbf{n}_v(k)\tilde{\mathbf{y}}_v^H(k)\tilde{\mathbf{D}}_N\mathbf{D}_N(\omega_0)\mathbf{f}_N\left(\frac{2\pi i_t}{N}\right)\right)\right\} \\ &= \frac{2}{M}\Im\left\{\sum_{v=1}^{N_r}\sum_{k=0}^{M-1}\sum_{t=1}^{N-K}\left(\mathbf{f}_N^H\left(\frac{2\pi i_t}{N}\right)\mathbf{D}_N^{-1}(\omega_0)\tilde{\mathbf{D}}_N\tilde{\mathbf{y}}_v(k)\mathbf{n}_v^H(k)\mathbf{D}_N(\omega_0)\mathbf{f}_N\left(\frac{2\pi i_t}{N}\right)\right)\right\} \end{aligned} \tag{5.16}$$

where $\tilde{\mathbf{D}}_N = diag(0,1,\ldots,N-1)$. And the denominator of (5.14) can be obtained by differentiating equation (5.16), before substituting ω with ω_0, with respect to ω as

$$\begin{aligned}
&\left.\frac{\partial^2 J(\omega)}{\partial \omega^2}\right|_{\omega=\omega_0} \\
&= \frac{-j}{M}\left\{\begin{array}{l} -j\sum_{\upsilon=1}^{N_r}\sum_{k=0}^{M-1}\sum_{t=1}^{N-K}\left(\mathbf{f}_N^H\left(\frac{2\pi i_t}{N}\right)\mathbf{D}_N^{-1}(\omega_0)\tilde{\mathbf{D}}_N^2\mathbf{A}_\upsilon\mathbf{D}_N(\omega_0)\mathbf{f}_N\left(\frac{2\pi i_t}{N}\right)\right) \\ +j\sum_{\upsilon=1}^{N_r}\sum_{k=0}^{M-1}\sum_{t=1}^{N-K}\left(\mathbf{f}_N^H\left(\frac{2\pi i_t}{N}\right)\mathbf{D}_N^{-1}(\omega_0)\tilde{\mathbf{D}}_N\mathbf{A}_\upsilon\tilde{\mathbf{D}}_N\mathbf{D}_N(\omega_0)\mathbf{f}_N\left(\frac{2\pi i_t}{N}\right)\right)\end{array}\right\} \\
&\quad \frac{+j}{M}\left\{\begin{array}{l} -j\sum_{\upsilon=1}^{N_r}\sum_{k=0}^{M-1}\sum_{t=1}^{N-K}\left(\mathbf{f}_N^H\left(\frac{2\pi i_t}{N}\right)\mathbf{D}_N^{-1}(\omega_0)\tilde{\mathbf{D}}_N\mathbf{A}_\upsilon\tilde{\mathbf{D}}_N\mathbf{D}_N(\omega_0)\mathbf{f}_N\left(\frac{2\pi i_t}{N}\right)\right) \\ +j\sum_{\upsilon=1}^{N_r}\sum_{k=0}^{M-1}\sum_{t=1}^{N-K}\left(\mathbf{f}_N^H\left(\frac{2\pi i_t}{N}\right)\mathbf{D}_N^{-1}(\omega_0)\mathbf{A}_\upsilon\tilde{\mathbf{D}}_N^2\mathbf{D}_N(\omega_0)\mathbf{f}_N\left(\frac{2\pi i_t}{N}\right)\right)\end{array}\right\} \\
&= \frac{2}{M}\left\{\sum_{\upsilon=1}^{N_r}\sum_{k=0}^{M-1}\sum_{t=1}^{N-K}\left(\mathbf{f}_N^H\left(\frac{2\pi i_t}{N}\right)\mathbf{D}_N^{-1}(\omega_0)\tilde{\mathbf{D}}_N\mathbf{A}_\upsilon\tilde{\mathbf{D}}_N\mathbf{D}_N(\omega_0)\mathbf{f}_N\left(\frac{2\pi i_t}{N}\right)\right)\right\} \\
&\quad -\frac{2}{M}\Re\left\{\sum_{\upsilon=1}^{N_r}\sum_{k=0}^{M-1}\sum_{t=1}^{N-K}\left(\mathbf{f}_N^H\left(\frac{2\pi i_t}{N}\right)\mathbf{D}_N^{-1}(\omega_0)\tilde{\mathbf{D}}_N^2\mathbf{A}_\upsilon\mathbf{D}_N(\omega_0)\mathbf{f}_N\left(\frac{2\pi i_t}{N}\right)\right)\right\} \qquad (5.17)
\end{aligned}$$

where $\mathbf{A}_\upsilon = \mathbf{y}_\upsilon(k)\mathbf{y}_\upsilon^H(k)$. By substituting (5.15) in (5.17), we obtain

$$\begin{aligned}
&\left.\frac{\partial^2 J(\omega)}{\partial \omega^2}\right|_{\omega=\omega_0} \\
&= \frac{2}{M}\left\{\sum_{\upsilon=1}^{N_r}\sum_{k=0}^{M-1}\sum_{t=1}^{N-K}\left(\mathbf{f}_N^H\left(\frac{2\pi i_t}{N}\right)\mathbf{D}_N^{-1}(\omega_0)\tilde{\mathbf{D}}_N\mathbf{y}_\upsilon(k)\mathbf{y}_\upsilon^H(k)\tilde{\mathbf{D}}_N\mathbf{D}_N(\omega_0)\mathbf{f}_N\left(\frac{2\pi i_t}{N}\right)\right)\right\} \\
&\quad -\frac{2}{M}\Re\left\{\sum_{\upsilon=1}^{N_r}\sum_{k=0}^{M-1}\sum_{t=1}^{N-K}\left(\mathbf{f}_N^H\left(\frac{2\pi i_t}{N}\right)\mathbf{D}_N^{-1}(\omega_0)\tilde{\mathbf{D}}_N^2\tilde{\mathbf{y}}_\upsilon(k)\mathbf{n}_\upsilon^H(k)\mathbf{D}_N(\omega_0)\mathbf{f}_N\left(\frac{2\pi i_t}{N}\right)\right)\right\}. \qquad (5.18)
\end{aligned}$$

At high SNR, $\|\mathbf{n}_\upsilon\| \ll \|\tilde{\mathbf{y}}_\upsilon\|$, the perturbation parts of the first term $(\tilde{\mathbf{y}}_\upsilon(k)\mathbf{n}_\upsilon^H(k) + \mathbf{n}_\upsilon(k)\tilde{\mathbf{y}}_\upsilon^H(k) + \mathbf{n}_\upsilon(k)\mathbf{n}_\upsilon^H(k))$, together with the second term of (5.18), are much smaller than the useful part of the first term $\tilde{\mathbf{y}}_\upsilon(k)\tilde{\mathbf{y}}_\upsilon^H(k)$ and can be neglected. So the perturbation can be simplified as

$$\Delta\omega = \frac{\Im\left\{\sum_{v=1}^{N_r}\sum_{k=0}^{M-1}\sum_{t=1}^{N-K}\left(\mathbf{f}_N^H\left(\frac{2\pi i_t}{N}\right)\mathbf{D}_N^{-1}(\omega_0)\tilde{\mathbf{D}}_N\tilde{\mathbf{y}}_v(k)\mathbf{n}_v^H(k)\mathbf{D}_N(\omega_0)\mathbf{f}_N\left(\frac{2\pi i_t}{N}\right)\right)\right\}}{\sum_{v=1}^{N_r}\sum_{k=0}^{M-1}\sum_{t=1}^{N-K}\left(\mathbf{f}_N^H\left(\frac{2\pi i_t}{N}\right)\mathbf{D}_N^{-1}(\omega_0)\tilde{\mathbf{D}}_N\tilde{\mathbf{y}}_v(k)\tilde{\mathbf{y}}_v^H(k)\tilde{\mathbf{D}}_N\mathbf{D}_N(\omega_0)\mathbf{f}_N\left(\frac{2\pi i_t}{N}\right)\right)}. \quad (5.19)$$

Then we compute the expectation of the error $(\Delta\omega)^2$, which is the theoretical MSE of the estimator. In order to simplify the equation, we set

$$\alpha_{t,k}^{v} = \mathbf{f}_N^H\left(\frac{2\pi i_t}{N}\right)\mathbf{D}_N^{-1}(\omega_0)\tilde{\mathbf{D}}_N\tilde{\mathbf{y}}_v(k). \quad (5.20)$$

Then, the squared error of estimator is given by [46]

$$(\Delta\omega)^2 = \frac{\sum_{v,\bar{v}=1}^{N_r}\sum_{k,\bar{k}=0}^{M-1}\sum_{t,\bar{t}=1}^{N-K}\left(\begin{array}{l}\Im\left(\alpha_{t,k}^{v}\mathbf{n}_v^H(k)\mathbf{D}_N^{-1}(\omega_0)\mathbf{f}_N\left(\frac{2\pi i_t}{N}\right)\right)\times \\ \Im\left(\mathbf{f}_N^H\left(\frac{2\pi i_{\bar{t}}}{N}\right)\mathbf{D}_N(\omega_0)\mathbf{n}_{\bar{v}}(\bar{k})\left(\alpha_{\bar{t},\bar{k}}^{\bar{v}}\right)^*\right)\end{array}\right)}{2\sum_{v,\bar{v}=1}^{N_r}\sum_{k,\bar{k}=0}^{M-1}\sum_{t,\bar{t}=1}^{N-K}\left(\alpha_{t,k}^{v}\left(\alpha_{t,k}^{v}\right)^*\alpha_{\bar{t},\bar{k}}^{\bar{v}}\left(\alpha_{\bar{t},\bar{k}}^{\bar{v}}\right)^*\right)}. \quad (5.21)$$

The numerator of (5.21) consists of the noise and the required data, while the denominator only includes the required data. Since the data and the noise are independent of each other, we can calculate their expectations separately. The theoretical MSE can be expressed as

$$\begin{aligned}
&E\left[(\Delta\omega)^2\right] \\
&= E\left\{\frac{Symbol\,E[Noise]}{Symbol}\right\} \\
&= E\left\{\frac{\sum_{v,\bar{v}=1}^{N_r}\sum_{k,\bar{k}=0}^{M-1}\sum_{t,\bar{t}=1}^{N-K}\left(\alpha_{t,k}^{v}E\left(\mathbf{n}_v^H(k)\mathbf{D}_N^{-1}(\omega_0)\mathbf{f}_N\left(\frac{2\pi i_t}{N}\right)\mathbf{f}_N^H\left(\frac{2\pi i_{\bar{t}}}{N}\right)\mathbf{D}_N(\omega_0)\mathbf{n}_{\bar{v}}(\bar{k})\right)\left(\alpha_{\bar{t},\bar{k}}^{\bar{v}}\right)^*\right)}{2\sum_{v,\bar{v}=1}^{N_r}\sum_{k,\bar{k}=0}^{M-1}\sum_{t,\bar{t}=1}^{N-K}\left(\alpha_{t,k}^{v}\left(\alpha_{t,k}^{v}\right)^*\alpha_{\bar{t},\bar{k}}^{\bar{v}}\left(\alpha_{\bar{t},\bar{k}}^{\bar{v}}\right)^*\right)}\right\} \\
&= E\left\{\frac{\sigma_{\mathbf{n}}^2\sum_{v=1}^{N_r}\sum_{k=0}^{M-1}\sum_{t=1}^{N-K}\left(\alpha_{t,k}^{v}\left(\alpha_{t,k}^{v}\right)^*\right)}{2\left(\sum_{v=1}^{N_r}\sum_{k=0}^{M-1}\sum_{t=1}^{N-K}\alpha_{t,k}^{v}\left(\alpha_{t,k}^{v}\right)^*\right)^2}\right\} = E\left[\frac{\sigma_{\mathbf{n}}^2}{2\sum_{v=1}^{N_r}\sum_{k=0}^{M-1}\sum_{t=1}^{N-K}\left|\alpha_{t,k}^{v}\right|^2}\right].
\end{aligned} \quad (5.22)$$

In Eqn. (5.22), the denominator, which only includes unperturbed data, is unknown but deterministic. So we use the sample covariance matrix obtained from M realizations to represent the expectation of this part. Substituting the expression of received block $\tilde{\mathbf{y}}_{\upsilon}(k) = e^{j\omega_0(kP+L)}\mathbf{D}_N(\omega_0)\sum_{\mu=1}^{N_t}\tilde{\mathbf{H}}^{(\upsilon,\mu)}\mathbf{F}_N^H\mathbf{T}_{SC}\mathbf{s}_{\mu}(k)$ into (5.22), leads to

$$E[(\triangle\omega)^2] \approx \frac{\sigma_{\mathbf{n}}^2}{2\sum_{\upsilon=1}^{N_r}\sum_{k=0}^{M-1}\sum_{t=1}^{N-K}\left|\mathbf{f}_N^H\left(\frac{2\pi i_t}{N}\right)\tilde{\mathbf{D}}_N\mathbf{g}_{\upsilon}(k)\right|^2} \tag{5.23}$$

where $\mathbf{g}_{\upsilon}(k) = \sum_{\mu=1}^{N_t}\tilde{\mathbf{H}}^{(\upsilon,\mu)}\mathbf{F}_N^H\mathbf{T}_{SC}\mathbf{s}_{\mu}(k)$.

5.5 Computational Complexity

In the previous section, we mentioned that the main purpose of the proposed estimation method is to reduce the computational cost without sacrificing performance. In this section, we show how this is achieved.

Let us first discuss the computational cost when we use equations (5.8) to estimate the CFO. From equation (5.7), we can see that the computational complexity of the correlation matrix $\widehat{\mathbf{R}}_{\mathbf{yy}}$ is $O(N_rMN^2)$. The derivative of the original polynomial (5.8) requires $O((N-K)(3N^2+N))$ complex multiplications. Since $N-K \ll N$, the complexity of this part becomes only $O(N^2)$. We use a search method to find the minimum of equation (4.7). We assume that there are S samples of ω, the search process requires a complexity of $O(2(N-1)S)$, which can be simplified to $O(SN)$ for $S \gg N$. So the total computational complexity of the first method, which requires high cost, is $O(N^2)+O(SN)+O(N_rMN^2)$.

For the proposed estimation algorithm, we derive the polynomial coefficients from equations (5.10) and (5.13). The computational complexity is $O(2(N^2+N)MN_r(N-K)Q^2)$. Since $N-K \ll N$ and $N \gg Q$, it can be simplified to $O(N^2MN_r)$. On the other hand, the complexity of rooting method depends only on Q, which can be neglected. If we also use a search method, then the complexity will be $O((2Q+1)S)$. Therefore, the computational complexity of the proposed method is about $O(N^2MN_r)+O(S)$, or only $O(N^2MN_r)$. In the original and proposed methods, the computation of the correlation matrix $\widehat{\mathbf{R}}_{\mathbf{yy}}$ is inevitable, which will cause a computational complexity of $O(N^2MN_r)$. So the cost reduction can only be performed in the searching stage. Compared with the original estimator, the complexity of the proposed estimator in the searching stage can be neglected if we use the rooting method to find the CFO estimate. It is clear that the proposed method reduces the computational cost significantly.

5.6 Simulation Results

In this section, we show the simulation and analytical MSE results of two cases of the MIMO multicarrier system: MIMO-OFDM and MIMO MC-CDMA. QPSK modulation and Rayleigh fading channels are used in the simulation. We assume that the channel order is $L=3$ and choose $N=32$. The estimated correlation matrix $\hat{\mathbf{R}}_{\mathbf{y}_v}$ is averaged across M=320 blocks. The carrier offset is $\omega_0 = 0.1\varpi$. For MIMO MC-CDMA systems, the spreading sequences are taken from the orthogonal Hadamard matrix.

5.6.1 Simulation Results for MIMO-OFDM system

MIMO-OFDM is a typical MIMO multicarrier system. There is only one user at the transmit side. The spreading code $\mathbf{c}_\mu^\nu = [c_\mu^\nu(0)\ c_\mu^\nu(1)\cdots c_\mu^\nu(K-1)]^T$ is, in this case, a k-element unit vector. It means that the blocks $\left\{\mathbf{t}_\mu^\nu(k)\right\}_{\mu=1}^{N_t}$ are just passed through an S/P converter. In the simulations, we choose $K=27$ to be the number of information symbols in each transmitted block.

Fig. 5.2 gives the results for different number of antennas with the proposed method for $Q=2$. At low SNR, the MSE decays rapidly. But, the slope of the curves decreases when SNR increases. In general, we can notice that the system performance improves when the number of antennas increases. Compared with the theoretical MSE, which is obtained on the conditions that $N_t = N_r = 3$, the performance of proposed method is acceptable for practical application.

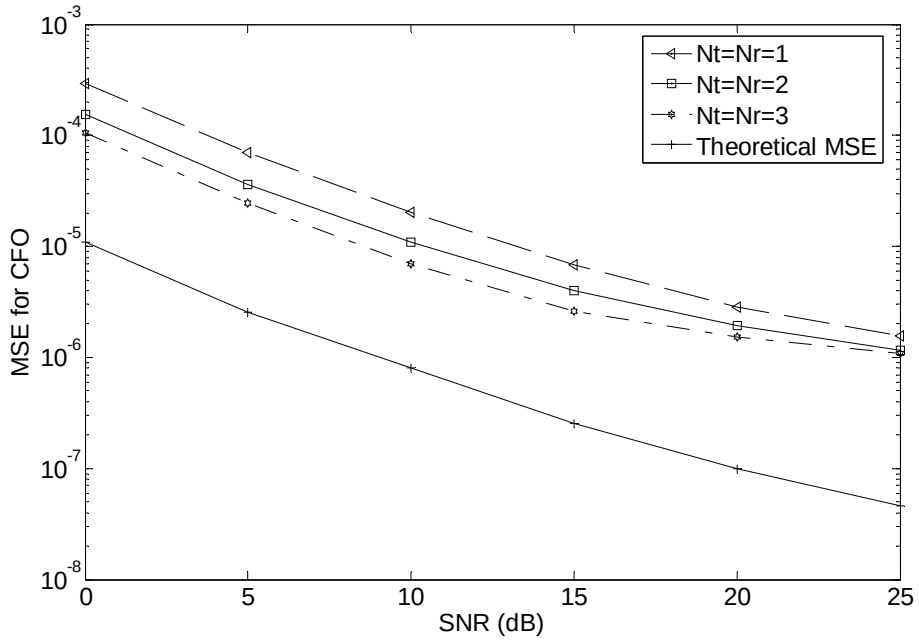

Fig. 5.2: MSE of CFO estimation for MIMO-OFDM system using the proposed method for $Q=2$, $\omega_0 = 0.1\varpi$.

Fig. 5.3 compares the result of the high-cost method with the proposed one when the number of antennas $N_t = N_r = 3$. When $Q = 1$, the performance at low SNR is not good. It seems that the truncation error is too large. But when SNR>20dB, the results of both methods are comparable. On the other hand, the performance of the proposed method is very good at low SNR with $Q = 2$. This phenomenon, which also appears in SISO systems, will be discussed in the next section.

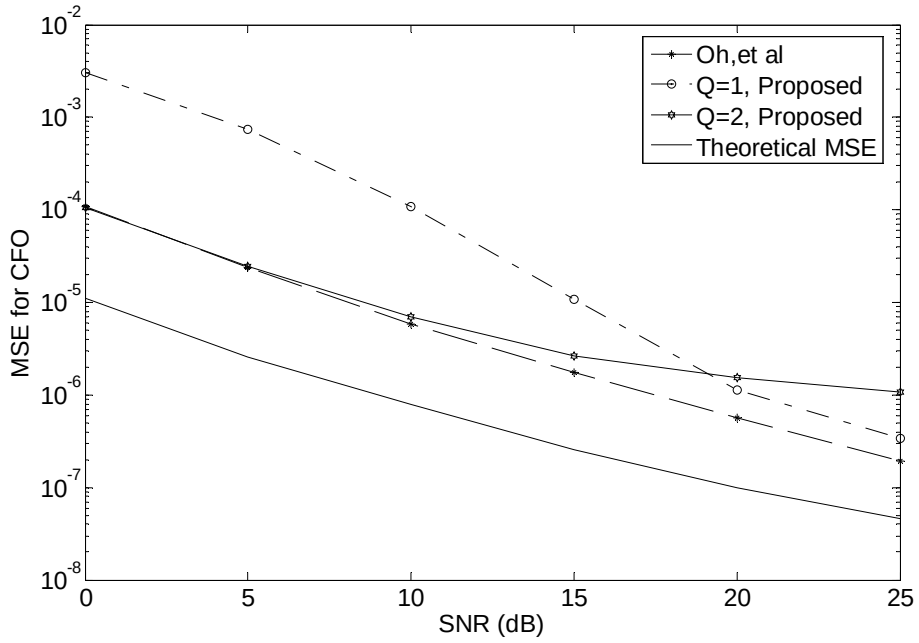

Fig. 5.3: MSE of CFO estimation for MIMO-OFDM system using both the proposed and Oh et al [44] methods, $N_t = N_r = 3$ and $\omega_0 = 0.1\varpi$

5.6.2 Simulation Result for MIMO MC-CDMA system

Down-link MIMO MC-CDMA system is a combination of MIMO-OFDM and MC-CDMA system. At the transmitter, the data stream $\left\{t_\mu^\nu(k)\right\}_{\mu=1}^{N_t}$ of the $\nu - th$

user is replicated by copiers. Each data bit of the $\nu-th$ user is multiplexed with a specific spreading code $\mathbf{c}_\nu^\mu = [c_\nu^\mu(0)\ c_\nu^\mu(1)\cdots c_\nu^\mu(K-1)]^T$, which is one column of the orthogonal Hadamard matrix. Because the length of the spreading code is K, the maximum number of users is $N_u(\max) = \lfloor K / N_t \rfloor$.In our simulations, we select $K = 24$ as in Chapter 4.

Fig. 5.4 shows the performance of the proposed method when the carrier frequency offset $\omega_0 \in [-0.5\varpi\ \ 0.5\varpi]$. SNR and the number of antennas and number of users are the same for every case. We observe that when $Q = 1$, the low-cost method cannot estimate CFO accurately unless ω_0 is very close to zero. If $\omega_0 \in [-0.1\varpi\ \ 0.1\varpi]$, the performance of the proposed method with $Q = 2$ is as good as the high-cost one. We can choose $Q = 3$ when the CFO $\omega_0 \in [-0.3\varpi\ \ 0.3\varpi]$. It is because that the larger the CFO, the more terms of the Taylor's series are needed for estimation.

Fig. 5.5 compares the result of the high-cost method [44] with the proposed one when the number of antennas $N_t = N_r = 3$. It is clear that when $SNR > 25$, the results of $Q = 1$ and $Q = 2$ converge to a limit, which have been mentioned in Chapter 4. If we use the Taylor's series expansion for an exponential function, we should expect the accuracy of our representation to increase as we increase the terms we retain in the Taylor's series. However, in this case, the Taylor's series is embedded into a complex system with multiple access interference due to many reasons, such as multiuser access, multiple antennas and the interference of noise. All these are interacting together in a very complex way and it is not easy to separate their effects

in order to know about these phenomena.

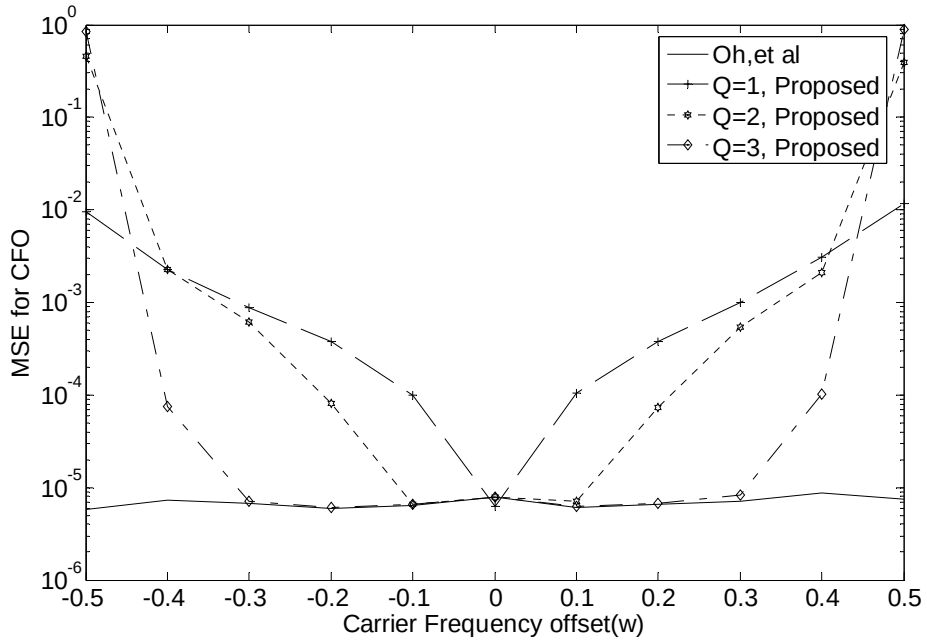

Fig. 5.4: MSE of CFO estimation for MIMO MC-CDMA system using both the proposed and Oh et al [44] methods,

$SNR = 10$, $N_t = N_r = 3$, $N_u = 8$, and $\omega_0 \in [-0.5\varpi \;\; 0.5\varpi]$

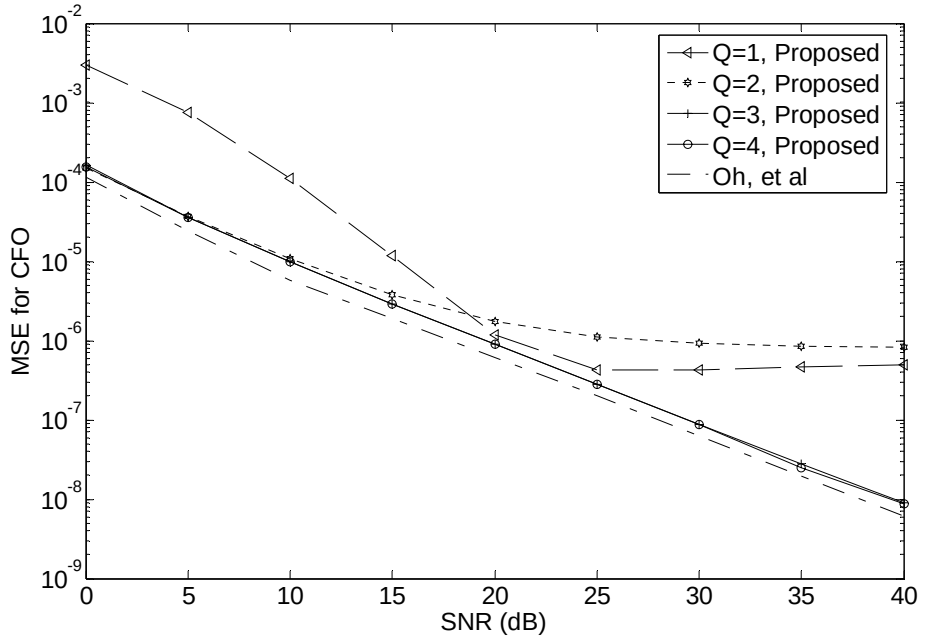

Fig. 5.5: MSE of CFO estimation for MIMO MC-CDMA system using both the proposed and Oh et al [44] methods, $N_t = N_r = 3$ and $\omega_0 = 0.1\varpi$

Fig. 5.6 gives the results when the CFO ω_0 is varied uniformly over the interval $[-0.125\varpi \;\; 0.125\varpi]$. Similar to Fig. 5.3, when $Q=1$, the performance at low SNR is not good. But the result for $Q=2$ is comparable to the high-cost one. We expand from the results shown in Fig. 5.4, and demonstrate in Fig. 5.6 that the proposed method with $Q=2$ is able to estimate the CFO very accurately when $\omega_0 \in [-0.1\varpi \;\; 0.1\varpi]$. In Fig. 5.6 and Fig. 5.7, theoretical MSE is presented to show that the performance of our low-cost algorithm is quite good.

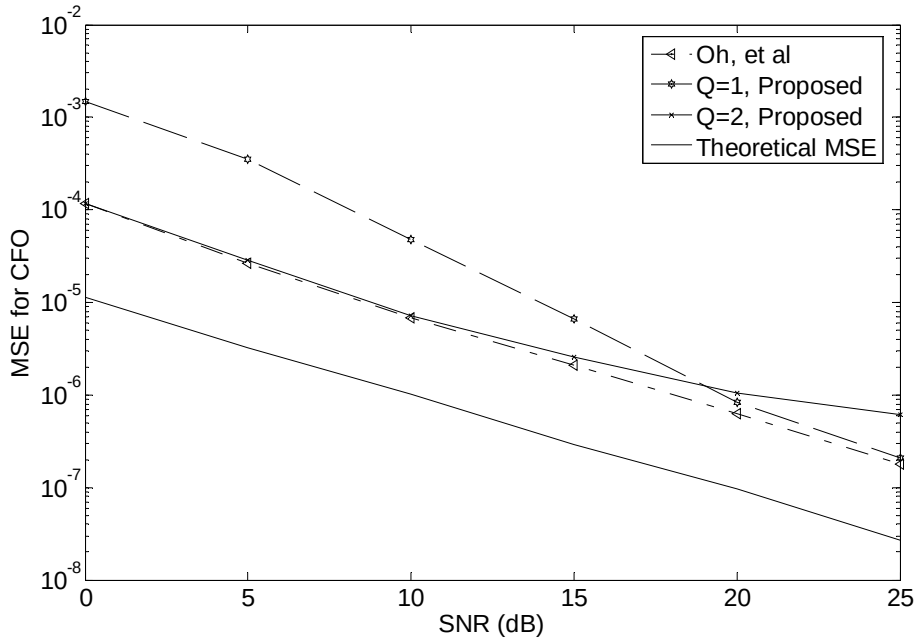

Fig. 5.6: MSE of CFO estimation for MIMO MC-CDMA system using both the proposed and Oh et al [44] methods,

$N_t = N_r = 3$, and $\omega_0 \in [-0.125\varpi \;\; 0.125\varpi]$

Fig. 5.7 compares the performance of the proposed method with different number of antennas. We can find that no matter how many antennas there are at the transmit side, the results remain the same for the same number of receive antennas. In other words, the performances of the estimator only depend on the number of receive

antennas. It can be explained by equation (5.6), which shows that only the number of receive antennas will effect the accuracy of the covariance matrix $\mathbf{R}_{yy}$.

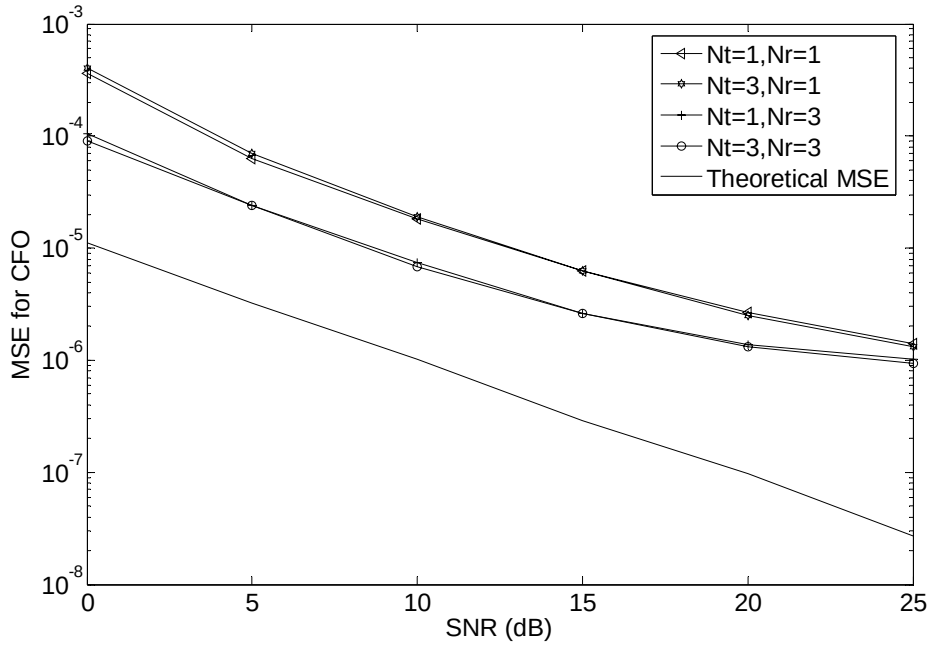

Fig. 5.7: MSE of CFO estimation for MIMO MC-CDMA system using the proposed method for $Q = 2$, $\omega_0 = 0.1\varpi$, and different number of antennas

Fig. 5.8 shows the performance when the number of antennas increases. We set $SNR = 10$ while using the extended method from [44] and the proposed method. It is clear that the performance is enhanced with an increase in the number of antennas. We also observe that the results of $Q = 3$ is not much better than that of $Q = 2$, which justifies the conclusion that when $\omega_0 \in [-0.1\varpi \ 0.1\varpi]$, $Q = 2$ is adequate for estimation.

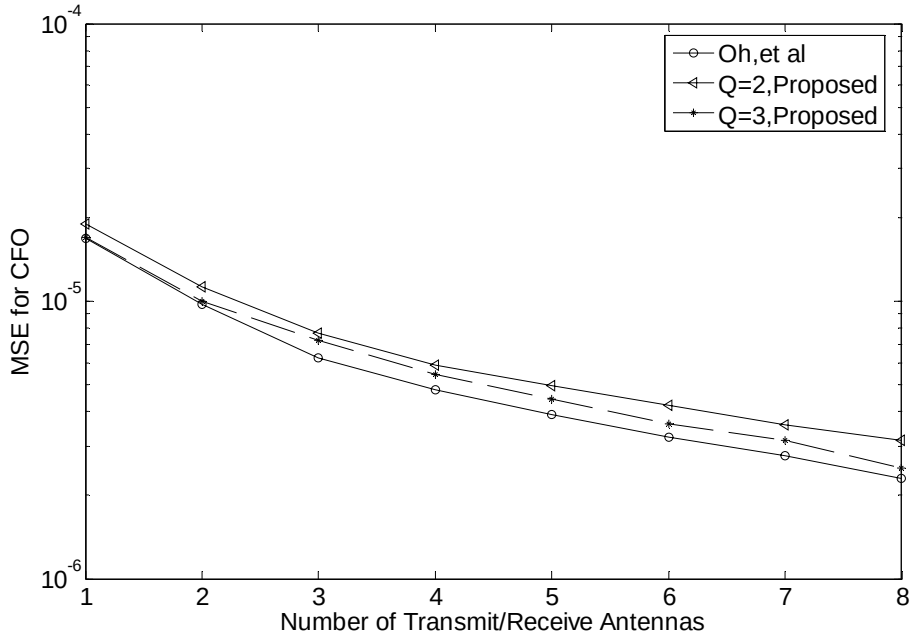

Fig. 5.8: MSE of CFO estimation for MIMO MC-CDMA system using both the proposed and Oh et al [44] methods, $\omega_0 = 0.1\varpi$ and $SNR = 10$

From the simulation results, we notice that under similar conditions, the performance of MIMO multi-carrier systems is better than SISO systems. This is because in SISO system, $\mathbf{R}_{\mathbf{yy}}$ is estimated by $\widehat{\mathbf{R}}_{\mathbf{yy}} = \frac{1}{M}\sum_{k=0}^{M-1}\mathbf{y}(k)\mathbf{y}^H(k)$, while in MIMO systems, $\mathbf{R}_{\mathbf{yy}}$ is estimated as $\widehat{\mathbf{R}}_{\mathbf{yy}} = \frac{1}{M}\sum_{\upsilon=1}^{N_r}\sum_{k=0}^{M-1}\mathbf{y}_\upsilon(k)\mathbf{y}_\upsilon^H(k)]$, which equals to averaging across $N_r M$ blocks. The larger the number of receive antennas, the more precise the estimation of the covariance matrix in MIMO systems is. Therefore, the performance of the system is enhanced as the number of antennas increases.

5.7 Summary

In this chapter, the low-cost blind CFO estimation method is extended to MIMO

multicarrier system. We discuss in detail how the proposed method reduces the computational cost. In the simulation, two typical cases of multicarrier system are presented. From the numerical results, we can find that the parameter Q determines the performance. When the CFO ω_0 increases, the parameter Q must be increased to retain the accuracy of the estimator. On the other hand, the performance of the estimator is enhanced with increase in the number of antennas.

Chapter 6

Conclusions and Future Work

6.1 Conclusions

Multicarrier systems have received much attention in recent years and are widely used in wireless communications. The principle of a multicarrier system is to divide the channel bandwidth into several narrowband sub-channels. The main advantages of multicarrier systems are high data rate, high bandwidth efficiency and robustness against frequency selective fading. The inter-symbol interference (ISI) can be eliminated using a time-guard or a cyclic prefix. The performance of multicarrier system has been proven to be significantly better than a single-carrier system. OFDM, which is a typical case of multicarrier system, has been adopted by many standards (e.g., IEEE 802.11a, IEEE 802.11g, and HIPERLAN/2). Multicarrier system is considered as a promising technique for WLANs, broadcasting and so on.

On the other hand, MIMO transmission is considered to be a potential technique to satisfy the high demand for data rate, which is required by the development of WLANs. It has been demonstrated that the capacity and bit error rate are enhanced significantly by increasing the number of antennas. As the combination of two techniques, MIMO multicarrier system offers high data rate, high bandwidth efficiency, robustness to frequency-selective fading and so on. So the MIMO

multicarrier system is considered as a promising technique for high speed wireless communication in the future.

Although multicarrier system has many advantages, it is very sensitive to carrier frequency offset (CFO). CFO destroys the orthogonality among the subcarriers, causes ICI and degrades the BER performance severely. Therefore, the estimation and compensation of CFO is very important to OFDM system. In recent years, a number of CFO estimation methods were proposed. These existing CFO estimators can be classified into two groups: one is data-aided, whereas the other is non-data-aided or blind estimators.

As its name implies, data-aided estimators use pilot symbols or training symbols to estimate the CFO. Although data-aided estimators have good performance, pilot symbols and training symbols occupy considerable bandwidth. As a result, the blind CFO estimation methods have received much attention for their high bandwidth efficiency. There are several classes of blind estimators, which respectively make use of null subcarriers, cyclic prefix, correlation of received signals and so on.

In these blind estimators, the ones which use null subcarriers were studied in this thesis. A polynomial cost function based on null subcarriers is constructed in these algorithms, and the CFO estimate is the value which minimizes this cost function. Because of the high computational complexity of this approach, some new algorithms have been proposed to reduce the cost. Besides that, the identifiability problem has been resolved by locating null subcarriers in different ways, too.

In this thesis, we proposed a low-cost blind CFO estimation algorithm for MIMO

multi-carrier system based on the use of null subcarriers. The identifiability problem is also considered. We compare the computational cost of the proposed method with former method and show how the proposed method reduces the cost. The simulation results of four cases show that the performance of the proposed method is comparable to the high-cost ones.

6.2 Future Work

The new low-cost estimator is an effective method to estimate the CFO for multicarrier systems. But the range of the CFO, which can be estimated precisely, is not wide. From the simulation results, we can find that the proposed method is suitable for estimation of decimal part of the CFO. When the CFO increases, the parameter Q must be increased to ensure the accuracy of the estimate, and the computational cost increases consequently. It means that when the CFO is large, the truncation error of the proposed method is too large. So a new approximate form of the cost function has to be found to estimate the large CFO.

Bibliography

[1] T. S. Rappaport, *Wireless Communications: Principles and Practice*, Prentice Hall Inc, 2002, Chapters 1 & 2.

[2] P. Nicopolitidis, M. S. Obaidat, G. I. Papadimitriou and A. S. Pomportsis, *Wireless Networks*, John Wiley &Sons, Ltd, 2003, Chapter 1.

[3] S. Hara and R. Prasad, *Multicarrier Techniques for 4G Mobile Communications*, Artech House, 2003, Chapters 1 & 3.

[4] C. R. Nassar, B. Natarajan, Z. Wu, D. Wiegandt, S. A. Zekavat and S. Shattil, *Multi-carrier Technologies for Wireless Communication*, Kluwer Academic Publishers, 2002, Chapter 2.

[5] J. Bingham, "Multicarrier modulation for data transmission: an idea whose time has come," *IEEE Comm. Mag*., vol. 28, no. 5, pp. 982-989, May 1990.

[6] T. J. Willink and P. H. Wittke, "Optimization and performance evaluation of multicarrier transmission," *IEEE Trans. Inform. Theory*, vol. 43, pp. 24, Mar. 1997.

[7] L. Hanzo et al., *OFDM and MC-CDMA for broadcasting multi-user communications, WLANs and Broadcasting*, Wiley, 2003, Chapter 1.

[8] A. J. Paulraj et al., "An overview of MIMO communications: A key to gigabit wireless," *Proc. IEEE*, vol. 92, no. 2, pp. 198-218, Feb. 2004.

[9] G. L. Stuber, J. R. Barry, S. W. McLaughlin, L. Ye, M. A. Ingram and T. G. Pratt, "Broadband MIMO-OFDM wireless communications," *Proc. IEEE*, vol. 92, issue 2, pp. 271-294, Feb. 2004.

[10] H. Yang, "A road to future broadband wireless access: MIMO-OFDM-Based air interface," *IEEE Comm. Mag.*, vol. 43, issue 1, pp. 53-60, Jan. 2005.

[11] S. Alamouti, "A simple transmit diversity technique for wireless communications," *IEEE J. Select. Areas Comm.*, vol. 16, pp. 1451–1458, Oct. 1998.

[12] V. Tarokh, N. Seshadri and A. R. Calderbank, "Space–time codes for high data rate wireless communication: Performance criterion and code construction," *IEEE Trans. Inform. Theory*, vol. 44, pp. 744–765, Mar. 1998.

[13] P. W. Wolniansky, G. J. Foschini, G. D. Golden and R. A. Valenzuela, "V-Blast: An architecture for realizing very high data rates over the rich-scattering channel," *Proc. Int. Symp. Signals, Systems and Electronics (ISSE 1998)*, pp. 295–300.

[14] M. A. Beach, D. P. McNamara, P. N. Fletcher and P. Karlsson, "MIMO-a solution for advanced wireless access," *11th IEE International Conference on Antennas and Propagation*, vol. 1, Apr. 2001, pp. 231-235.

[15] R. V. Nee and R. Prasad, *OFDM for Wireless Multimedia Communication*, Artech House Publishers, 2000, Chapters 2 & 4.

[16] H. Liu and U. Tureli, "A high-efficiency carrier estimator for OFDM communications," *IEEE Comm. Letters*, vol. 2, no. 4, pp.104-106, Apr. 1998.

[17] R. R. Mosier and R. G. Clabaugh, “KINEPLEX, a bandwidth-efficient binary transmission system,” *AIEE Trans*., vol. 76, pp. 723-728, Jan. 1958.

[18] M. S. Zimmerman and A. L. Kirsch, “The AN/GSC-10 (KATHRYN) variable rate data modem for HF radio,” *IEEE Trans. Comm. Tech*., vol. COM-15, pp. 197-205, Apr. 1967.

[19] H. F. Marmuth, “On the transmission of information by orthogonal time functions,” *AIEE Trans.*, vol. 79, pp. 248-255, Jul. 1960.

[20] “Orthogonal Frequency Division Multiplexing,” U. S. Patent No. 3,488,445, Filed Nov. 14, 1966, Issued Jan. 6, 1970.

[21] N. Yee, J. P. Linnartz and G. Fettweis, “Multicarrier CDMA in indoor wireless radio networks,” *Proc. IEEE PIMRC’93*, Yokohama, Japan, Sep. 1993, pp. 109-113.

[22] K. Fazel and L. Papke, “On the performance of Convolutionally-Coded CDMA/OFDM for mobile communication system,” *Proc. IEEE PIMRC’93*, Yokohama, Japan, Sep. 1993, pp. 468-472.

[23] A. Chouly, A. Brajal and S. Jourdan, “Orthogonal multicarrier techniques, applied to direct sequence spread spectrum CDMA systems,” *Proc. IEEE GLOBECOM’93*, Houston, TX, Nov. 1993, pp. 1723-1728.

[24] Y. Wu and W. Y. Zou, “Orthogonal frequency division multiplexing: a multi-carrier modulation scheme,” *IEEE Trans. Consumer Electronics*, vol. 41, no. 3, pp. 392-398, Aug. 1995.

[25] S. B. Weinstein and P. M. Ebert, “Data transmission by frequency division

multiplexing using the discrete Fourier transform," *IEEE Trans. Comm. Tech.*, vol. COM-19, no. 15, Oct. 1971.

[26] E. Bidet et al., "A fast 8K FFT VLSI ship for large OFDM single frequency networks," *Proc. Intl. Conf. on HDTV 94*, Turin, Italy, Oct. 1994.

[27] D. Castelain, "Analysis of interfering effects in a single frequency network," CCETT report, Sep. 1989.

[28] S. Hara and R. Prasad, "Overview of multicarrier CDMA," *IEEE Comm. Magazine*, vol. 35, issue 12, pp. 126-133, Dec. 1997.

[29] S. Hara, T-H. Lee and R. Prasad, "BER comparison of DS-CDMA and MC-CDMA for frequency selective fading channels," *Proc. 7th Tyrrhenian International Workshop on Digital Comm.*, Viareggio, Italy, Sept. 1995, pp. 3-14.

[30] T. Pollet, M. V. Bladel and M. Moeneclaey, "BER sensitivity of OFDM systems to carrier frequency offset and Wiener phase noise," *IEEE Trans. Comm.*, vol. 43, pp. 191-193, Feb./Mar./Apr. 1995.

[31] T. M. Schmidl and D. C. Cox, "Robust frequency and timing synchronization for OFDM," *IEEE Trans. Comm.*, vol. 45, no. 12, pp. 1613-1621, Dec. 1997.

[32] K. Sathananthan and C. Tellambura, "Performance analysis of an OFDM system with carrier frequency offset and phase noise," *Proc. IEEE VTC*, 54th, Atlantic City, NJ, vol.4, Oct. 2001, pp. 2329-2332.

[33] K. Sathananthan and R. M. A. P. Rajatheva, "Analysis of OFDM in the presence of frequency offset and a method to reduce performance degradation," *Proc. IEEE Globecom*, San Francisco, CA, vol. 1, Nov. 2000, pp. 72-76.

[34] G. Proakis, *Digital Communications*, McGraw Hill, Inc, 1995, Chapter 2.

[35] P. H. Moose, "A technique for orthogonal frequency division multiplexing frequency offset correction," *IEEE Trans. Comm.*, vol. 42, pp. 2908-2914, Oct. 1994.

[36] Y. S. Lim and J. H. Lee, "An efficient carrier frequency offset estimation scheme for an OFDM system," *Proc. of VTC 2000 Fall*, vol. 5, Sept. 2000, pp. 2453-2457.

[37] M. Li and W. Zhang, "A novel method of carrier frequency offset estimation for OFDM systems," *IEEE Trans. Consumer Electronics*, vol. 49, no. 4, pp 965-972, Nov. 2003.

[38] J. J. van de Beek, M. Sandell and P. O. Borjesson, "ML estimation of time and frequency offset in OFDM systems," *IEEE Trans. Signal Processing*, vol. 45, pp. 1800-1805, Jul. 1997.

[39] T. Roman and V. Koivunen, "Blind CFO estimation in OFDM systems using diagonality criterion," *2004 IEEE International Conference on Acoustics, Speech, and Signal Processing*, vol. 4, 2004, pp. 369-372.

[40] B. Chen and H. Wang, "Blind OFDM carrier frequency offset estimation via oversampling," *Signals, Systems and Computers, 2001. Conf. Record of the 35th Asilomar Conf.*, vol. 2, Nov. 2001, pp. 1465-1469.

[41] S. Attallah, "Blind estimation of residual carrier offset in OFDM systems," *IEEE Signal Processing Letters*, vol. 11, no. 2, pp. 216-219, Feb. 2004.

[42] X. Ma et al. "Non-data-aided carrier offset estimators for OFDM with null

subcarriers: Identifiability, algorithms, and performance," *IEEE Journal selected areas in Comm*. vol.19, no.12, pp. 2504-2515, Dec. 2001.

[43] U. Tureli, H. Liu and M. D. Zoltowski, "OFDM blind carrier offset estimation: ESPRIT," *IEEE Trans. Comm*. vol. 48, no. 9, pp. 1459-1461, Sept. 2000.

[44] M. Oh, X. Ma, G. B. Giannakis and D. Park, "Hopping pilots for estimation of frequency-offset and multi-antenna channels in MIMO OFDM," *Proc. IEEE Globecom*, vol. 2, Dec. 2003, pp. 1084-1088.

[45] X. Ma, M. Oh, G. B. Giannakis and D. Park, "Hopping pilots for estimation of frequency-offset and multiantenna channels in MIMO-OFDM," *IEEE Trans. Comm.*, vol. 53, issue 1, pp. 162-172, Jan. 2005.

[46] U. Tureli, D. Kivand and H. Liu, "Experimental and analytical studies on a high-resolution OFDM carrier frequency offset estimator," *IEEE Trans. Vehicular Technology*, vol. 50, issue 2, pp. 629-643, Mar. 2001.

[47] X. Wu, Q. Yin and Y. Zeng, "Downlink channels identification for space-time coded multiple-input multiple-output MC-CDMA systems," *Proc. IEEE ICASSP'03*, vol. 4, Apr. 2003, pp. 417-420.

List of Publications

[1] M. Li, A. Nallanathan and S. Attallah, “Blind Carrier Estimation for MIMO MC-CDMA Systems with Low Complexity,” *International Symposium on Signal Processing and Its Applications (ISSPA) 2005*, vol. 1, Aug. 2005, pp. 127-130.

[2] M. Li, A. Nallanathan and S. Attallah, “A Low-cost Blind Carrier Offset Estimator for MIMO-OFDM Systems,” *IEEE Military Communication Conference (MILCOM) 2005 Proceedings*, Oct. 2005, pp. 1-5.

[3] M. Li, S. Attallah and A. Nallanathan, “A Low-cost Blind Carrier Frequency Offset Estimator for Down-link MIMO Multicarrier Systems,” accepted by *IEE Proc. Communications*.